# Diagnosing Spatial Policies in a Changing Commons

Karl M. Aspelund and Aaron Berman*

June 15, 2026

**Abstract**

How does the value of spatial regulation change as ecological variability increases due to climate change? We develop a framework that decomposes the regulator's recursive problem into three structurally distinct efficiency conditions—intratemporal, spatial, and intertemporal—while allowing for spatial substitution, heterogeneous ecological shocks, and distributional concerns. Applied to detailed ecological and harvest data in the U.S. Atlantic sea scallop fishery, we find that the existing set of closures, harvest limits in certain areas, and day restrictions is too lax overall and has substantial spatial misallocation of harvests. Leakage destroys about 17% of the marginal value of future conservation but dampens the marginal cost of conservation today even more, increasing the static inefficiency of the overall policy. The regulations, meanwhile, implicitly under-value the resource stock year to year. Climate-induced changes in the resource amplifies each type of inefficiency, though slowing mean growth versus increasing variance and spatial correlation of ecological shocks play varying roles. The existing regulation can be rationalized statically by rather moderate inequality aversion and dynamically by a regulator using out-dated expectations over the level and correlation of resource growth over space.

*Aspelund: Harvard Center for the Environment, karlaspelund@fas.harvard.edu. Berman: MIT, bermana@mit.edu.

# 1 Introduction

Regulators tasked with managing an ecologically important resource face pronounced spatial heterogeneity and substantial uncertainty over future changes in ecological and economic conditions. Examples occur across environmental economics: a forest agency deciding which compartments to harvest and at what intensity under disturbances like wildfire and insect outbreaks; fire managers setting fuel-management strategies across large areas; a fishery manager setting quotas across spatial grounds where warming oceans change growth trajectories; a water board allocating extraction rights across basins under drought variability; or an air-quality regulator pricing emissions across locations with spatially differentiated damages. In each case the underlying problem has the same structure: biology or geophysics is uncertain, the resource is unevenly distributed across cells, firms substitute their activity across space, and the environment is changing in ways that move multiple moments of the natural process simultaneously. Across all these commons problems, climate change makes future ecological change more uncertain, and the relationship between regulatory design and welfare becomes harder to characterize. This paper develops a framework for evaluating spatial environmental policy under uncertainty and an empirical exercise that evaluates a changing ocean's impact on the value of a spatial management in the U.S. Atlantic sea scallop fishery.

How does the value of spatial regulation change as ecological variability increases? We set up tests based on an extension of the canonical natural resource problem with multiple areas, producers substituting across space, and ecological and economic uncertainty. It focuses on a regulator maximizing social welfare by managing production across areas with varying private production profits as well as environmental benefits that depend negatively on the level of production. Moreover the environmental benefits can change over time, are uncertain, and can spill over into other areas (e.g. fire risk, pollution, or resource growth). It decomposes into three structurally distinct efficiency conditions, each of which calls for a different reform. The first is an intratemporal condition and asks if there is inefficient harvest in that area: today's rent (the marginal profit at the restricted harvest i.e. the marginal cost of conservation) should equal the discounted future stock-value benefit of conserving the marginal unit (the marginal benefit of conservation). The second is a spatial condition across areas: at the optimum, the ratio of the marginal cost of conservation to the marginal benefit should be the same across space. The third is an intertemporal condition: the shadow value should evolve according to a modified Hotelling rule that allows for changes in production in one area to impact others (leakage). The conditions are set ex ante, considering a distribution of states, and can allow

for flexible social welfare functions by the planner. One can evaluate the efficiency of a spatial policy under stationarity versus the observed changes in the resource over time.

Importantly, the framework considers non-optimal policies and particularly the welfare consequences of spatial substitution of production, often called leakage (Fowlie and Muller 2019; Reynaert, Souza-Rodrigues, and van Benthem 2023). Leakage—whether from general-equilibrium price adjustments or incomplete regulation—does not have a fixed welfare sign, and the sign is set by the spatial correlation of the environment. Displaced activity can be a *hedge* when it flees to whatever place happens to be slack (insurance) and a *hazard* when everything is stressed at once. If the spatial correlation of environmental shocks changes, the welfare consequences of leakage can change dramatically, even for a fixed policy. The major sources of inefficiency (and therefore reform) might then be not excessive laxity nor misallocation but a *failure to update*, a policy optimally targeted for ecological conditions that no longer exist. It could then change which areas are most important to target for spatial policies, given spillovers and changing conditions.

We apply this framework to the U.S. Atlantic sea scallop fishery, among the most valuable fisheries in the country and one of the most carefully monitored renewable-resource systems in the world. Regulator set patch-level harvest caps in rotating access areas, an aggregate days-at-sea (DAS) constraint that is not tradable across vessels, and full closures of patches with high growth potential. Given the close monitoring, we are able to match detailed harvest data across the ocean with annual biomass surveys that count scallop beds as well as their size, capturing important quality distinctions often missing from even terrestrial resources. The US East Coast is among the fastest-warming ocean regions in the world, generating shifting mean growth, growing marginal variance, and rising spatial covariance in the underlying biology. Trip-level vessel positions and landings, size-class-specific landings and prices, independent biomass surveys, and the assessment model's structural biology by management subarea together permit identification of each of the framework's diagnostics separately. We first document a set of reduced-form regularities that motivate the structural choices: vessels reallocate across space in response to regulatory status; access-area caps on quantities bind tightly in practice while days-at-sea in open areas binds loosely; and harvest is strongly responsive to local biomass. These regularities discipline the structural choices and pin down behavioral parameters that the counterfactual exercise relies on.

We then specify a structural model of fleet choice and biology (a nested-logit choice model over (area, trip-day) combinations, size-structured stock dynamics with patch-specific recruitment shocks, and an estimated catch production function with decreasing

returns to biomass). This allows us to recover ex-ante value and uncover different mechanisms driving inefficiency. Within this calibrated structure, a marginal-harvest perturbation experiment recovers the cap rent, the dynamic shadow value of stock, and the cross-patch leakage matrix at each access area. The actual closures, openings, and day/harvest limits are held fixed across the period.

The perturbations let us test the three conditions in turn. *Statically*, the regulation is too lax if the goal is to maximize harvest profit over time: summed across areas, the marginal benefit of conservation exceeds the marginal cost by roughly 60%, with wide variation across patches, the largest open-water grounds sometimes under-harvested, several access areas over-harvested, and the 2014 closures valuable enough that closing them is efficient. The targeting of which areas to close is roughly right even though the permitted level is too lax. Leakage cuts the marginal benefit of conservation by about 17% (a binding aggregate days-at-sea constraint means extra harvest in one patch crowds out effort elsewhere) but cuts the marginal cost by more, so on net it raises the static inefficiency by about 13%. Decomposing the spatial misallocation, about 73% is between patches and only 10% between boats, suggesting that differentiating the allowed caps or otherwise managing the spatial inefficiency is more important than misallocation of production across boats a priority ordering opposite to the standard tradable-quota recommendation. *Dynamically*, the regulation's implicit pricing of in-water stock fails the costate (Euler) condition under observed biomass growth: the residual is strongly positive, so the stock is worth more than the regulator's revealed shadow value implies.

Taking account of inequality concerns changes the conclusions. The static wedge crosses zero at moderate inequality aversion ($p \approx 1.5$ in Table 10), because the conservation gains accrue disproportionately to high-revenue boats from the largest New England ports rather than to less profitable Mid-Atlantic vessels; a planner who weights the latter more heavily sees the regulation's distributional pattern as offsetting its static laxness. And while the dynamic residual shrinks under inequality aversion—in line with the static wedge shrinking—it stays positive at every plausible preference: even a planner who rationalizes the 2014 stringency on equity grounds is not updating enough to be robust going forward.

The central exercise isolates the role of a changing ocean by holding the mean, variance, and covariance of biomass shocks at early-period values and re-estimating against the late-period values. Each condition responds to a different moment. The aggregate static wedge widens, driven mainly by rising variance and spatial correlation: more variable and more synchronized shocks raise the option value of stock left in the water. Spatial inefficiency worsens, driven mainly by slowing Mid-Atlantic mean growth, though

the rising correlation compresses the dispersion of $\mathrm{MB}/\mathrm{MC}$. And the dynamic residual is almost entirely a mean-growth phenomenon: under frozen growth and correlation it is indistinguishable from zero, so the dynamic failure is a failure to update to slowing biomass, not static laxity propagated forward.

Beyond its effect on each separate condition, the changing ocean changes the consequences of leakage itself. We measure the welfare sign of leakage directly, as the flow-weighted covariance between where displaced harvest goes and how stressed those destinations are. Under the early-period biology this covariance is essentially zero and mildly negative: displaced effort fled to whichever grounds happened to be slack (where scallops were plentiful), so leakage was a hedge. Under the observed late-period biology it turns sharply positive, a sign flip rather than a larger number, because warming synchronizes the grounds, so that when shocks hit everywhere at once the few productive destinations are also the high-conservation-value ones and displaced effort floods the patches least able to absorb it. The flip is regional, emerging in the southern, fastest-warming Mid-Atlantic while the already-synchronized northern grounds barely move. Climate has thus made the leakage concern qualitatively worse: a leakage rate estimated at historical correlation does not merely understate leakage in a warmer future, it gets the sign of its state-dependence wrong.

Future work will incorporate ecological leakage (how environmental benefits themselves depend on other areas) and consider how far the existing instruments (closures, changing access limits, day restrictions) can be adjusted to increase efficiency across the three tests. Then we will turn to more ambitious regulatory reforms, ones that might manage leakage better and others that are robust to the non-stationary nature of the resource: what designs maintain resource value *ex ante* across the range of climate trajectories? This question pervades environmental regulation and can inform regulatory design and instrument choice across resource issues.

In so doing, we hope to offer a framework useful to analyze spatial policies across many environmental domains like habitat protection, pollution management, or deforestation. Massive disturbances like wildfire, pests, and floods are highly uncertain and quickly changing as the world warms, meaning that the precautionary value of protecting some areas can change and the value of principles outlining policies robust to those concerns is important.

**Related literature.** Our central contribution is to show that the welfare sign of spatial policies, and particularly the substitution of production induced by those policies, is not a property of the policy but of the spatial correlation structure of the environment, and

that climate change moves it from hedge to hazard, reframing a well-documented phenomenon into one with a testable climate prediction. We develop a framework that decomposes the regulator's recursive optimization into three structurally distinct efficiency conditions (intratemporal, spatial, and intertemporal) each diagnosable separately and each mapping to a different reform when violated, with the corollary that the first failure to look for is often a stale spatial map rather than laxity. We provide empirical evidence on spatial substitution, binding constraints, and the cross-vessel and cross-patch structure of misallocation in a major rotational management program; and we use a structural model to diagnose each efficiency condition, decompose its sensitivity to climate and to distributional preferences, and rank competing reform levers through a variance decomposition of the underlying misallocation.

The paper builds on foundational work in renewable-resource economics on optimal harvesting under uncertainty (Reed 1979; Clark 1990; Pindyck 1984; Weitzman 2002; Pizer 2002), which established the precautionary value of stocks, and on the robust-control tradition that recently has come to focus on optimal climate policies (Hansen and Sargent 2008; Brock and Hansen 2018). We build on these by separating the dynamic problem into its three constituent first-order conditions, each empirically distinguishable to deliver clear policy implications.

We contribute to the empirical literature on fisheries management, which evaluates catch shares (Costello et al. 2008), effort limits (Essington et al. 2012), and spatial management tools (White and Costello 2014), often focusing on average effects. We instead produce a diagnostic structure for which margins the regulation actually fails, and complement work on the distributional impacts of environmental policy (Ryan 2019; Sudarshan 2020) by showing that the directional reading of the regulation's static-efficiency failure is planner-specific while the dynamic-efficiency failure is not.

We connect to literature on spatial policies under displacement and spillovers (Reynaert, Souza-Rodrigues, and van Benthem 2023; Earle Grupp et al. 2023; Souza-Rodrigues 2019; Assunção, Gandour, and Souza-Rodrigues 2019; Assunção et al. 2022) and on leakage in emissions regulation (Fowlie and Muller 2019; Goulder and Stavins 2011). That work establishes that activity relocates when restricted; our point is to show that the relocation's welfare sign is itself the object of interest, is set by spatial correlation, and moves with changing ecological conditions. This work is not focused on uncertainty, and how varying ecological and economic shocks change the welfare consequences of leakage or spaial restrictions generally.

Our framing is motivated by climate risk in natural-resource systems. Climate change alters expected ecological productivity, variance, and spatial correlation of ecological shocks

in spatially differentiated ways (Pinsky and Mantua 2014; Free et al. 2019; Mills et al. 2013). Our framework makes the link between these moments and the three efficiency conditions explicit. The insurance-versus-contagion mechanism connects to the portfolio view of conservation (Markowitz 1952; Mallory and Ando 2014; Holland 2010), where diversification across imperfectly correlated assets lowers risk; we show that the same correlation structure governs whether *leakage* hedges or amplifies risk, and that warming erodes the diversification a spatial policy implicitly relied on. Rather than evaluating portfolios as a whole, we identify which condition a regulation fails, attribute the failure to a specific moment of the shock distribution, and map to a specific reform lever.

# 2 Framework: spatial regulation under uncertainty

We study a regulator who manages a spatially distributed environmental benefit with a coarse, spatially differentiated policy, facing a mass of agents who reallocate activity across space in response and an environment whose shock distribution drifts over time. "Activity" is harvest, development, extraction, or emission; the "benefit" is a fish stock, a standing forest, habitat, an aquifer, or clean air; and "leakage" is the reallocation of activity that any binding restriction induces. The argument that follows holds for all of these, so we develop it on general primitives and return to the fishery only in the empirical sections. Full derivations, the size-structured generalization, and the welfare-weighted extension are in Appendix A.

The whole section is organized around a single object, the *static wedge* $\Delta_k \equiv \mathrm{MC}_k - \mathrm{MB}_k$: the gap, at area $k$, between what the regulator forgoes by restricting a unit of activity and the discounted, network-inclusive damage that unit would have done. Efficiency is a set of statements about this wedge — that it is zero at each area, equal in ratio form across areas, and stable as the regulator updates the policy over time. Because the regulator commits to the policy before shocks realize, the relevant wedge is an *expectation*, and the central conceptual content of the section is what enters that expectation: first leakage (Section 2.5), which routes other areas' wedges into $k$'s, then uncertainty (Section 2.6), which adds two covariances, then a drifting environment (Sections **??**–2.7), which lands on each margin differently. We build the wedge up one force at a time, beginning without space at all.

## 2.1 Setup

Areas $k = 1, \ldots, K$ in discrete time $t$. At each area an activity level $q_{k,t}$ yields a private return $\pi_k(q_{k,t}, B_{k,t}, \eta_{k,t})$ and degrades a socially valued environmental benefit $B_{k,t}$ worth $v_k(B_{k,t})$, with economic shocks $\eta$ and ecological shocks $\varepsilon$. The benefit's law of motion couples the areas,

$$B_{k,t+1} = G_k(\mathbf{B}_t, \mathbf{q}_t, \varepsilon_{k,t+1}), \qquad \partial G_k/\partial q_{k,t} < 0 \quad \text{(activity degrades the benefit)}, \tag{1}$$

and two derivatives of $G$ carry its spatial structure: own persistence $G_{k,k} \equiv \partial G_k/\partial B_{k,t}$ and the *ecological spillover* $G_{j,k} \equiv \partial G_j/\partial B_{k,t}$, positive for dispersal or recharge and negative for a spreading hazard such as fire or pest. Ecological shocks are drawn from $\varepsilon_{t+1} \sim F_\varepsilon(\cdot; \theta_t)$, whose mean, variance, and cross-area covariance $\theta_t$ encode the environment and its drift. The regulator maximizes expected discounted social value,

$$V(\mathbf{B}_t) = \max\ \mathbb{E} \sum_t \beta^t \sum_k \left[\pi_k(q_{k,t}, B_{k,t}, \eta_{k,t}) + v_k(B_{k,t})\right] \quad \text{subject to } (1), \tag{2}$$

with discount factor $\beta \in (0, 1)$. Environmental settings differ in which factors are most important to include. A *fishery* is the case $\pi_{k,B} > 0,\ v \approx 0$: the stock is valuable because it lowers future harvesting cost, with little amenity. A *pollution or development* externality might hae $\pi_{k,B} \approx 0,\ v' > 0$. A *wildfire* system is the corner where the spillover is negative, $G_{j,k} < 0$: protecting a stand raises the hazard it passes to its neighbors. A *water or aquifer* system has $G_{j,k} > 0$ through recharge.

The regulator does not solve (2) directly. It commits, before shocks realize, to a state-contingent rule $\mathbf{q}_t = \mathbf{h}(\mathbf{B}_t)$; activity then reacts to the realized state. The rule need not be optimal, and the point of the exercise is to measure, from observed behavior, how far it departs from optimality. Every diagnostic below is therefore evaluated *along the actual rule* $\mathbf{h}$, not at the planner's solution.

## 2.2 Two conditions before space

First we consider a single area, or many that do not interact, to fix two conditions in their simplest form.

**The static condition and the wedge.** Consider restricting a marginal unit of activity. The regulator forgoes the private return on that unit, a *marginal cost of restriction* $\mathrm{MC}_t \equiv \mathbb{E}_t[\pi_q]$, and gains the discounted future damage that unit would have done, a *marginal ben-*

*efit of restriction* $\mathrm{MB}_t \equiv -\beta\,\mathbb{E}_t[\lambda_{t+1}\,\partial G/\partial q]$, where $\lambda_t \equiv \partial V/\partial B_t$ is the costate, the marginal social value of the benefit. Static efficiency requires the wedge to close,

$$\Delta_t \;\equiv\; \mathrm{MC}_t - \mathrm{MB}_t \;=\; 0. \tag{3}$$

A lax rule leaves $\Delta_t < 0$ (the benefit is worth more left in place than the activity earns); an over-tight rule leaves $\Delta_t > 0$.

**The dynamic condition as an asset price.** The costate obeys an asset-pricing recursion and considers how the observed rule updates over time. Differentiating (2) and applying the envelope theorem, the condition at the optimal policy is

$$\lambda_t \;=\; d_t \;+\; \beta\,\mathbb{E}_t[\lambda_{t+1}\,G_B]\,, \qquad d_t \equiv \pi_B + v'(B_t), \tag{4}$$

where the *dividend* $d_t$ is the within-period value the benefit pays (private cost saving plus amenity) and $G_B$ is own persistence. The benefit therefore evolves according to a modified Hotelling rule, worth its dividend today plus the discounted value of what it persists into tomorrow.

**The relationship between static and dynamic conditions.** Equation (3) is a within-period level condition; (4) is a law of motion for the shadow value. They can be tested separately. Evaluate the costate recursion along the actual rule $h$ and collect the deviation into a realized residual, $u_t \equiv \lambda_t - d_t - \beta\,\mathbb{E}_t[\lambda_{t+1}G_B]$, with $\mathbb{E}[u_t] = 0$ at the optimum (a GMM-style Euler test in the sense of **?**). Under the actual rule the residual picks up the rule's responsiveness to the state, weighted by the static wedge:

$$\boxed{\mathbb{E}_t[u_{t+1}] \;=\; -\,\beta\,\mathbb{E}_t[\,h'(B_{t+1})\,\Delta_{t+1}\,G_B\,]\,.} \tag{5}$$

The dynamic test fails whenever the static one does: a non-zero wedge $\Delta$ propagates into the costate through the rule's slope $h'$. Dynamic inefficiency therefore inherits any static inefficiency, though a residual can survive *after* the static wedge is accounted, an important consideration if the ecological conditions underlying expectations can drift (Section **??**).

## 2.3 Allowing for spatial linkages

Now let the areas interact, both ecologically (through $G$) and economically (through the agents' shared environment). Two things change: the costate becomes a networked asset, and the policy acquires leakage.

**Introducing ecological "leakage".** With spillovers the recursion (4) gains cross-area terms,

$$\lambda_{k,t} \;=\; d_{k,t} \;+\; \beta\,\mathbb{E}_t\left[\lambda_{k,t+1}\,G_{k,k} \;+\; \sum_{j\neq k}\lambda_{j,t+1}\,G_{j,k}\right], \tag{6}$$

so a unit of benefit at $k$ is worth its dividend, plus what it persists into at $k$, plus what it *seeds in its neighbors* through $G_{j,k}$. Stacking across areas where $G$ is locally linear gives $\boldsymbol{\lambda} = (I - \beta\,\widetilde{G}^{\top})^{-1}\mathbf{d}$, with $\widetilde{G} = [G_{j,k}]$: the price of the benefit is its dividend propagated through the spatial network of who feeds whom. In a fishery that network runs through larval dispersal ($G_{j,k} > 0$); in a wildfire system the dominant terms are negative, and protecting a stand prices in the hazard it exports.

**Introducing spatial substitution ("leakage" of activity).** Restricting activity at one area shifts it elsewhere, through one of two channels. The first is *price-induced*: a binding restriction lowers aggregate activity, raises the common price $P(\sum_k q_k)$, and pulls activity into the unrestricted areas. The second is *regulation-induced*: a shared binding constraint — a commons-wide effort budget, a basin-wide water right, a sectoral emissions cap — couples the rule, so that the activity chosen at one area depends on the entire state vector, $\partial h_j/\partial B_k \neq 0$. Either channel makes $\mathbf{h}$ a genuinely spatial object; Section 2.5 constructs the resulting reallocation from primitives.

**Spatial efficiency: equalize ratios.** With a binding aggregate constraint, the regulator can move a unit of the scarce aggregate activity between areas at the margin. Efficiency then requires that the welfare gained per unit of that scarce activity be equalized across active areas, i.e. that the benefit-cost ratio be equal:

$$\frac{\mathrm{MB}_k}{\mathrm{MC}_k} \quad \text{equal across all active areas.} \tag{7}$$

The planner does *not* equalize the costates $\lambda_k$; areas with very different stocks optimally carry very different shadow prices. Conditioning on active areas allows for the fact that full closures can be optimal if $\mathrm{MB}_k > \mathrm{MC}_k$ even at zero activity.

## 2.4 Three diagnostic conditions

The framework therefore delivers three structurally distinct efficiency diagnostics, each necessary for full dynamic optimality, each able to fail independently, and each sensitive to a different moment of $\theta_t$.

| Diagnostic | Test | Object |
|---|---|---|
| Static intratemporal | $\Delta_k = 0$ at each area | level of the wedge |
| Static spatial | $\mathrm{MB}_k/\mathrm{MC}_k$ equal across areas | dispersion of the wedge |
| Dynamic intertemporal | $\mathbb{E}[u_{k,t}] = 0$ along the path | wedge propagated through the costate |

The intratemporal test assesses the *level* of the wedge area by area; the spatial test assesses its *equality* (in ratio form) across areas; the intertemporal test assesses the wedge *propagated forward* through the costate's law of motion. The rest of the section focuses on how substitution and uncertainty affect these three conditions.

## 2.5 Leakage and the wedge

Next, we show how leakage affects the welfare effects of spatial policy.

**Constructing the reallocation.** Take the transparent case of a shared binding budget (effort, quota, or emissions), $\sum_k q_k \le \bar{T}$, with multiplier $\mu \ge 0$, though the intuition carries over for any source of spatial substitution. Each active agent equates private marginal return to the common shadow price, $\pi_{j,q}(q_j, B_j) = \mu$. When the regulator removes one unit of activity at $k$, the freed budget redistributes so as to keep the constraint binding. Differentiating the agents' first-order conditions, $\pi_{j,qq}\, dq_j = d\mu$, together with $\sum_{j\neq k} dq_j = 1$, gives the share of the displaced unit that lands at $j$,

$$\ell_{jk} \;\equiv\; \frac{\partial q_j^\star}{\partial(\text{unit restricted at } k)} \;=\; \frac{1/\pi_{j,qq}}{\sum_{i\neq k} 1/\pi_{i,qq}} \;\ge\; 0, \qquad \sum_{j\neq k} \ell_{jk} = 1 \,(\text{binding}), \quad \ell_{jk} = 0 \,(\text{slack}). \tag{8}$$

Activity flows toward the areas that absorb it most elastically (flattest marginal return). The price-induced channel yields an $\ell_{jk}$ of the same form, built from the demand slope and the agents' cost curvatures; the full derivation of both is in Appendix A.5. When the aggregate constraint does not bind, or there are no price effects, $\ell_{jk} = 0$ and there is no leakage.

**Relation between wedges.** Restricting at $k$ now has two muted margins. The forgone profit is partly *recovered* where the activity reappears, so the marginal cost falls to $\mathrm{MC}_k = \mathrm{MC}_k^{\text{own}} - \sum_{j\neq k} \ell_{jk}\, \mathrm{MC}_j^{\text{own}}$; and the avoided damage is partly re-created elsewhere, so the marginal benefit falls to $\mathrm{MB}_k = \mathrm{MB}_k^{\text{own}} - \sum_{j\neq k} \ell_{jk}\, \mathrm{MB}_j^{\text{own}}$. Therefore the overall wedge in any area can be decomposed into the own-area wedge of $k$ and its destinations:

$$\boxed{\Delta_k \;=\; \Delta_k^{\text{own}} \;-\; \sum_{j\neq k} \ell_{jk}\, \Delta_j^{\text{own}}, \qquad \Delta_j^{\text{own}} \equiv \mathrm{MC}_j^{\text{own}} - \mathrm{MB}_j^{\text{own}}.} \tag{9}$$

The leakage-inclusive wedge at $k$ (i.e. the overall static inefficiency) is its own wedge minus the leakage-weighted wedges of the places its displaced activity goes.

**Welfare consequences of leakage.** Equation (9) carries the entire welfare content of leakage in one term. A destination is *slack* when $\Delta_j^{\text{own}} > 0$ (activity there earns more privately than it damages, so restricting *it* would be unwarranted) and *stressed* when $\Delta_j^{\text{own}} < 0$. Leakage to a slack destination subtracts a positive quantity, pushing $\Delta_k$ down and making restriction at $k$ *more* warranted (lower marginal costs, higher marginal benefits): the activity escapes to a place that can absorb it. Leakage to a stressed destination subtracts a negative quantity, pushing $\Delta_k$ up: restriction merely shuffles harm onto an already over-exploited area. A regulator who ignores leakage therefore *understates* the case for restriction when destinations are slack and *overstates* it when they are stressed.

## 2.6 The expected wedge under uncertainty

Because the rule is fixed before shocks realize, every quantity in (9) is random, and the diagnostic is run on the *expected* wedge $\mathbb{E}[\Delta_k]$. It is uncertain how producers substitute across space, and this can change the effect.

**Own-area precaution, inside the marginal benefit.** The marginal benefit is itself an expectation of a product, the future costate times the marginal degradation. Uncertainty creates the standard precautionary value to conserving, increasing the value of restricting activity so as to prevent degraded sates in the future. Expanding,

$$\mathrm{MB}_k^{\text{own}} = \beta \sum_j \Big( \mathbb{E}[\lambda_{j,t+1}]\, \mathbb{E}\big[-\partial G_j/\partial q_k\big] + \underbrace{\mathrm{Cov}\big(\lambda_{j,t+1},\, -\partial G_j/\partial q_k\big)}_{\text{precautionary buffer}} \Big). \tag{10}$$

A positive buffer raises $\mathrm{MB}_k$ and so lowers $\Delta_k$. It is worth more when the area's future shadow value is high precisely in the states where degradation bites hardest. But the future shadow value is partially determined by existing regulation.

**Cross-area leakage, inside the reallocation term.** Both the reallocation $\ell_{jk}$ (which constraints bind depends on the realized state) and the destination wedge $\Delta_j^{\text{own}}$ (which depends on realized stocks) are random, so

$$\mathbb{E}\left[\sum_{j\neq k} \ell_{jk}\,\Delta_j^{\text{own}}\right] = \sum_{j\neq k}\Big(\mathbb{E}[\ell_{jk}]\,\mathbb{E}[\Delta_j^{\text{own}}] + \underbrace{\mathrm{Cov}\big(\ell_{jk},\,\Delta_j^{\text{own}}\big)}_{\text{the entire uncertainty effect on leakage}}\Big). \tag{11}$$

When activity tends to reroute toward areas that happen to be slack at the time ($\ell_{jk}$ high where $\Delta_j^{\text{own}}$ is high), the covariance is positive, the leakage term in (9) is larger, and restriction is reliably cheap. When reallocation and stress move together — $\ell_{jk}$ high exactly where $\Delta_j^{\text{own}}$ is low, — the covariance is negative and leakage delivers activity to the worst place at the worst time. It depends entirely on how sensitive spatial substitution is to price versus ecological shocks. Moreover, the spatial correlation of shocks is crucial: if areas become more stressed at the same time, then any sensitivity producers might have to ecological quality is dampened since all areas are degraded together.

## 2.7 How a changing environment moves each margin

Next, we consider changing ecological conditions. Climate change acts on $F_\varepsilon(\cdot;\theta_t)$ inside the expectations that define the wedge, the costate, and the two covariances above. Holding the existing policy fixed, there are the three moments of $\theta_t$ to consider:

| Moment of $\theta_t$ | Mechanism |
|---|---|
| Mean growth (drift) | $\lambda_{t+1}, G_{k,k}$ move first-order; stale beliefs (13) |
| Variance | precautionary buffer (10); amplifies leakage covariance |
| Correlation | sets sign of $\mathrm{Cov}(\ell_{jk}, \Delta_j^{\text{own}})$ (11); compresses $\mathrm{MB}_k/\mathrm{MC}_k$ |

*Mean growth* is the change in average benefit $B_k$ in any location, along with corresponding changes to ecological leakage across space. *Variance is a static problem* is the overall shock uncertainty and increases the precautionary value of conservation through (10). It also changes the strength of underlying leakage covariance. *Correlation* changes the spatial correlation of shocks and pushes $\mathrm{Cov}(\ell_{jk}, \Delta_j^{\text{own}})$ toward the unfavorable sign, since

synchronized shocks leave nowhere slack, while at the same time *compressing* the cross-area dispersion of $\mathrm{MB}_k/\mathrm{MC}_k$, because synchronized shocks make areas' precautionary responses more uniform.

**The dynamic residual: beliefs or pre-existing wedges?** The three changes above affect the size of the static wedge $\Delta_k$ directly, but we also want to touch on how it can separately feed into the dynamic inefficiency. This is to show that static inefficiency feeds into a dynamic one, but the dynamic test can fail even without considerable static inefficiency if regulators do not update the non-stationary process. The intertemporal diagnostic is the costate recursion (6) evaluated along the actual rule. Collecting the deviation,

$$u_{k,t} \;\equiv\; \lambda_{k,t} - d_{k,t} - \beta\,\mathbb{E}_t\Big[\lambda_{k,t+1}G_{k,k} + \textstyle\sum_{j\neq k}\lambda_{j,t+1}G_{j,k}\Big], \tag{12}$$

and taking expectations, the residual splits cleanly into a part inherited from static wedge and a part that is a genuine failure to update:

$$\mathbb{E}[u_{k,t}] = \underbrace{\sum_m \frac{\partial h_m}{\partial B_{k,t}}\,\mathbb{E}[\Delta_{m,t}]}_{\text{inherited: static wedges propagated (incl. leakage, } m\neq k)} + \underbrace{\beta\,(\widehat{\mathbb{E}}-\mathbb{E})\Big[\lambda_{k,t+1}G_{k,k} + \textstyle\sum_{j\neq k}\lambda_{j,t+1}G_{j,k}\Big]}_{\text{genuine: expectations lag a changing environment}}. \tag{13}$$

The inherited term is the multi-area version of the scalar result (5): a static wedge at $m$ is carried into $k$'s costate by the rule's state-responsiveness $\partial h_m/\partial B_{k,t}$, which for $m = k$ is own laxity and for $m \neq k$ is leakage. The genuine term arises when the regulator prices the benefit under stale beliefs $\widehat{\mathbb{E}}$, calibrated to a past climate, while the world evolves under the true $\mathbb{E}$. It does *not* vanish when the static wedges are zero, and because both $\lambda_{t+1}$ and the persistence factor $G_{k,k}$ move first-order with expected growth, it is driven mainly by *mean* drift.

The two terms are separately identified by freezing the environment. Under a frozen $\theta$ the genuine term is zero by construction, so any surviving residual is inherited static inefficiencies; a residual that *survives* stationarity is a genuine failure to update. Section 6.3 runs exactly this freeze-versus-evolve comparison.

## 2.8 Different SWFs

Throughout the conceptual framework we have assessed a regulator seeking to maximize the NPV of an environmental good, trading off productive activities for social environmental benefits. However, we can also consider distributional concerns. A welfare-

weighted generalization replaces the equal-weighted aggregator with $W = \sum_i w_i U(\pi_i)$ under CRRA utility $U(\pi) = \pi^{1-p}/(1-p)$, placing more weight on lower-revenue/profit/income agents as the inequality-aversion parameter $p$ rises.

The static condition then reweights by the marginal utility of profits at the areas where conservation gains concentrate. When those gains accrue disproportionately to high-revenue agents, an inequality-averse planner shrinks the wedge, allowing a lax regulation to be rationalized by protections for low-income groups. The dynamic condition reweights through the dividend $d_k$ and the forward costate $\lambda_{j,t+1}$, falling if the static wedge falls but nevertheless also affected by regulator's expectations.

A separate exercise could reveal implicit weights on different processors based on the regulatory design, understanding what weights across which characteristics could allow a regulation to have zero wedges.

# 3 Setting and Data

The U.S. Atlantic sea scallop fishery is the highest-revenue fishery on the U.S. East Coast and operates along the continental shelf from Virginia to Massachusetts. The fishery has three features that make it a stringent test setting for the framework. First, rotating closures—combined with "access areas" where harvests are restricted and an overall restriction on days at sea—allow for many events to understand the extent of regulation-induced spatial substitution and how sensitive it is to ecological and price shocks. Second, fleet substitution across spatial patches is observable in detail: trip-level vessel positions and landings are recorded for the full fleet from 2008 to 2022, with size-class-specific landings (the under-10 "u10" class commanding prices significantly above the smallest grades) and detailed homeport and vessel characteristics. Third, this region of the Atlantic is among the fastest-warming ocean regions in the world, with seafloor temperature shifts, recurring marine heatwaves (including a major event in 2012), and growing prevalence of gray-meat disease, generating shifts in mean recruitment, marginal variances, and cross-patch covariance in the underlying biology.

Two features of the regulatory instrument are important as sources of misallocation. The DAS allocation is non-tradable across vessels: boats whose DAS constraint binds tightly cannot acquire effort from boats whose constraint is slack, which is the source of the empirical leakage matrix (Section **??**) and the between-boat dispersion that an ITQ-style reform would compress. The access-area cap structure is spatially coarse: caps are set patch-by-patch by year, without fine-grained differentiation by underlying biological shadow value. A patch-level cap structure that responded more finely to local shadow

value would compress a different wedge. Section 6.1 quantifies both and delivers a sharp priority ordering. The Fisheries Management Council that sets these caps does so in advance of realized biology and prices, with the published Scallop Area Management Simulator (SAMS) providing biomass and size-distribution projections by management subarea; we use the SAMS panel directly in the structural exercise.

Climate change shifts three structurally relevant features of the biology process (mean recruitment, marginal variance of growth shocks, and the cross-patch covariance of those shocks) and the existing regulatory rule responds to none of them in a state-contingent way. The Mid-Atlantic, the southernmost and warmest part of the fishery, faces the largest changes: recruitment success has become more sensitive to local conditions across the range, and projections indicate continued warming with rising heatwave risk. Climate change alters the risk profile under which spatial policy operates, shifting the distribution and comovement of biological outcomes across space and time, which in turn changes the welfare value of different spatial regulatory configurations along each of the three efficiency conditions.

**Data.** We use NOAA Fisheries trip records (2008–2022), which contain daily landings by patch and size class with detailed vessel characteristics, location and timing of fishing activity, and homeport identifiers. These records are matched to NOAA biomass surveys generating spatially explicit estimates of scallop abundance and size structure, and to the rotational management system's record of which patches were closed, access, or open in each year (built from public NOAA shapefiles and digitized polygon coordinates from Federal Register announcements). Figure 1 maps the distribution of harvests and the constructed patch boundaries used in the location-choice model.

The structural model requires a patch-level, size-structured biomass panel, constructed as detailed in Section 5: published PDT/SAMS combined-survey totals by management subarea, allocated across patches by where the fleet actually fishes. This delivers patch biomasses consistent with the published totals and an exploitation rate ($F \approx 12\%$) matching the assessment, unlike earlier survey-sliver constructions that produced order-of-magnitude inconsistencies between patch biomass and observed catch. Institutional history (the regulatory timeline since 1982, the rotational schedule, the Council process, and auction-based price formation) and validation against the NOAA assessment are in separate setting and data appendices.

# 4 Reduced-form evidence

We document reduced-form regularities that motivate the structural choices in Section 5 and that each of the framework's structural objects will need to reproduce. Summary statistics on the sample are in Table 1.

We state the five estimating equations here and refer to them in the paragraphs that follow. Index vessels by $i$, areas (patches) by $k$, trips by $\tau$, and years by $t$. Let $R_{ikt}$ be vessel $i$'s status at area $k$ in year $t$, summarized by the indicators $\mathrm{Closed}_{kt}$ and $\mathrm{Access}_{kt}$ (the omitted category is open), and let $\mathrm{dist}_{ik}$ be the distance from $i$'s homeport to area $k$.

*(i) Trip-level location choice (conditional logit).* For trip $\tau$ by vessel $i$ in year $t$, the utility of choosing area $k$ from the regulation-varying choice set $\mathcal{C}_\tau$ is

$$U_{i\tau kt} = \beta_d \,\mathrm{dist}_{ik} + \gamma_C \,\mathrm{Closed}_{kt} + \gamma_A \,\mathrm{Access}_{kt} + \delta_t + \varepsilon_{i\tau kt}, \qquad \Pr(k \mid \mathcal{C}_\tau) = \frac{e^{U_{i\tau kt}}}{\sum_{k' \in \mathcal{C}_\tau} e^{U_{i\tau k' t}}}, \tag{14}$$

with $\delta_t$ year fixed effects and $\varepsilon$ i.i.d. type-I extreme value. The reported percentage effects are $e^{\gamma} - 1$ relative to open areas.

*(ii) Extensive margin (participation logit).* At the vessel-area-year level, the probability that $i$ fishes area $k$ at all in year $t$ is

$$\Pr(\mathrm{fish}_{ikt} = 1) = \Lambda\big(\beta_d^E \,\mathrm{dist}_{ik} + \gamma_C^E \,\mathrm{Closed}_{kt} + \gamma_A^E \,\mathrm{Access}_{kt} + \delta_t\big), \tag{15}$$

with $\Lambda$ the logistic c.d.f.

*(iii) Intensive margin (Poisson trip count).* Conditional on participation ($\mathrm{fish}_{ikt} = 1$), the trip count is

$$\mathbb{E}[n_{ikt} \mid \mathrm{fish}_{ikt} = 1] = \exp\big(\beta_d^I \,\mathrm{dist}_{ik} + \gamma_C^I \,\mathrm{Closed}_{kt} + \gamma_A^I \,\mathrm{Access}_{kt} + \delta_t\big). \tag{16}$$

Equations (15)–(16) decompose the conditional-logit response into whether vessels show up and how heavily they fish once present; standard errors are clustered at the vessel-year level.

*(iv) Spatial displacement (stacked event-study DiD).* Stacking regulatory events $e$ (closures, openings, access designations) and indexing $0.1^\circ$ cells $c$ by distance band $b(c, e) \in$ {event patch, 0–15, 15–50, 50–100, 100–200, $200+$ km} from the event patch, with event time $s = t - t_e$,

$$y_{cet} = \sum_{b} \sum_{s \neq -1} \theta_{b,s} \,\mathbf{1}[b(c,e) = b] \,\mathbf{1}[t - t_e = s] + \alpha_{ce} + \lambda_{et} + u_{cet}, \tag{17}$$

where $y_{cet}$ is trips, landings, or unique vessels; $\alpha_{ce}$ is a cell-by-event fixed effect; $\lambda_{et}$ is an event-by-year fixed effect; and $s = -1$ is the omitted base period. The displacement estimates plotted in Figure 2 are the $\widehat{\theta}_{b,0}$ across bands, normalized to the $200+$ km band as the clean comparison.

*(v) Biomass elasticity of harvest.* At the patch-year level,

$$\log H_{kt} = \eta \, \log B_{kt} + \eta_O \left( \log B_{kt} \times \text{Open}_{kt} \right) + \phi_k + \delta_t + \nu_{kt}, \tag{18}$$

with $H_{kt}$ harvest, $B_{kt}$ biomass, $\phi_k$ patch fixed effects, and $\eta_O$ the differential elasticity in the open regime; the test of regime invariance is $H_0 : \eta_O = 0$.

**Vessel choice responds strongly to regulatory status, on the extensive margin.** A conditional logit of trip-level location choice (eq. 14; Table 2) on the regulation-varying choice set finds that closure reduces the probability that an area is selected by approximately 49% relative to open areas, while access designation nearly doubles selection probabilities, conditional on a precisely estimated distance penalty. Decomposing into extensive and intensive margins (vessel-area-year participation logit and Poisson trip count conditional on participation), access designation increases the probability that a vessel fishes in an area by about 82%, while conditional trip counts barely move (a 2% point estimate, indistinguishable from zero). Closures cut participation by $\sim 69\%$ but leave conditional intensity unchanged. The behavioral channel through which spatial regulation operates is whether vessels show up at a patch, not how heavily they fish once present, a fact that disciplines the choice-diffuseness parameter in the structural model.

**Spatial substitution reaches 100–200 km, with no aggregate effect.** A stacked difference-in-differences across regulatory events (closures, openings, access-area designations; eq. 17), comparing $0.1^\circ$ cells in concentric distance bands from the affected patch, finds that closures generate sharp declines in activity within the treated patch with offsetting increases in nearby patches, largest in the 0–15 km band and statistically detectable to 100–200 km. Aggregate activity across bands is essentially unchanged: the fleet redistributes effort, it does not reduce or increase total effort, consistent with the binding aggregate DAS constraint that gives the framework's leakage matrix a non-trivial structure. Openings show mirror-image patterns. Figure 2 reports the event-study estimates.

**Leakage chases biomass, and spreads under high prices.** Displacement is not a constant rate; it responds to the state, which is what gives the structural leakage covari-

ance of Section 6.3 its bite. Interacting the recoup response (the post-event change in activity at nearby open donor patches, relative to the treated cell's loss) with destination pre-event biomass and event-year price (Table 3), two patterns hold across trips and harvest, at patch and boat level. Recoup rises monotonically with destination biomass: displaced effort chases the resource. And recoup into the immediate 0–50 km ring is *weaker* when prices are high: the fleet spreads effort further afield rather than piling into nearby grounds. The biomass pattern is the reduced-form shadow of the structural object (leakage flows to high-biomass destinations, which under synchrony are also the high-conservation-value ones) and is confirmed in the model in Section 6.3; the price pattern, which the fixed-price structural model cannot produce, runs opposite to the naive "higher price pulls harder locally" intuition. Donors are restricted to patches actually open, since roughly 40% of the raw 0–50 km ring is closed by the same event; without this the recoup response is spuriously negative.

**Access-area caps bind tightly; DAS in open areas binds loosely.** The distribution of annual trips to access areas, normalized by the modal regulatory threshold, exhibits a spike-to-baseline ratio exceeding $20\times$ at the limit, with similarly sharp bunching at the annual access-area harvest cap (Figure 3). The DAS distribution in open areas is smooth around its threshold with only modest excess mass at the cap. Two features of the institutional setting contribute: measurement error in recorded DAS (estimated from "days absent" rather than directly observed) and the empirical observation that vessels routinely do not exhaust their annual DAS allocation. The non-tradable structure means the aggregate constraint still binds at the vessel level for the high-shadow subset of the fleet ($\sim 60\%$); the cap shadow $\xi_k > 0$ assumed in the structural exercise is directly confirmed in the access-area trip distribution.

**Harvest is responsive to local biomass, with no regime differentiation.** Estimating year-over-year elasticity of harvest to biomass at the patch level (eq. 18) gives a baseline elasticity of 1.55 (s.e. 0.18) and an interaction with the open-regime indicator that is small and statistically indistinguishable from zero (implied open-regime elasticity 1.43, $p = 0.55$ for equality). The fleet's production response to ecological conditions does not differ across regulatory regimes. The reduced-form elasticity is an equilibrium object combining the production technology (the $\gamma < 1$ catch function in the structural model) with the fleet's endogenous response through entry and exit; the regime-invariance licenses the structural separation of biology process from regulation that makes the climate counterfactuals tractable.

These facts map onto the structural objects the framework distinguishes: the extensive-margin-dominant choice response calibrates the nested-logit model and the diffuseness parameter $\sigma$; the 100–200 km, aggregate-neutral displacement is the empirical analogue of the leakage matrix and disciplines $\sigma$ against the reduced-form reach; the bunching validates $\xi_k > 0$ at access patches; and the biomass elasticity establishes harvest's responsiveness to ecology, hence the importance of uncertainty.

# 5 Structural model

We implement the framework empirically with a nested-logit choice model of fleet behavior, a size-structured biology, a calibrated catch production function, and a marginal-harvest perturbation instrument that traces the Control FOC. Three foundational data fixes give the exercise credibility: the SAMS-anchored biomass panel, a Berry-style calibration of baseline area shares, and an explicit defense of the choice-diffuseness parameter against its naive estimate. Detailed parameter values, validation against the NOAA assessment, and sensitivity exercises are in a separate estimation appendix.

**Fleet behavior.** A nested-logit choice model generates vessel-level location choice, with trips choosing over (area, trip-day) alternatives nested by spatial cluster. For vessel $i$ on occasion $t$, the indirect payoff of the (area $k$, trip-day) alternative is

$$v_{ikt} = \beta_R \, \mathbb{E}[\mathrm{Rev}_{ikt}] - \beta_d \, \mathrm{dist}_{ik} - c_k - \mu_t \, \mathbf{1}[\text{DAS cap binds}] - \xi_{k,t} \, \mathbf{1}[\mathbb{E}[q_{ikt}] = \bar{q}_{kt}] + \delta_{mt} + \nu_{ikt}, \quad (19)$$

where $\mathbb{E}[\mathrm{Rev}_{ikt}]$ is expected revenue (observed prices times expected size-class catch), $c_k$ a mean area cost, $\delta_{mt}$ month-year fixed effects, and $\nu_{ikt}$ a nested type-I extreme-value shock with nest-correlation parameter $\omega_{\text{nest}}$ and scale $\sigma$. The two regulatory terms are the structural counterparts of the framework's multipliers: $\mu_t$ is the shadow value of the binding aggregate days-at-sea (DAS) budget and $\xi_{k,t}$ is the cap rent at access area $k$, recovered as the multipliers that rationalize observed catches against the DAS and per-patch caps. Choice probabilities follow the standard nested-logit form from (19). Behavioral parameters include the DAS shadow $\alpha$, the revenue response $\beta_R$, the distance cost $\beta_d$, Behavioral parameters include the DAS shadow $\alpha$, the revenue response $\beta_R$, the distance cost $\beta_d$, month-year fixed effects, and the nest-correlation $\omega_{\text{nest}}$; we use the estimated model in expectation, with aggregated choice probabilities at the boat-occasion level. The cap shadow $\xi_{k,t}$ and DAS shadow $\mu_t$ are the multipliers that rationalize observed catches against the per-patch caps and the aggregate DAS budget, mapping directly to the ves-

sel FOC in Section **??**. growth with patch-specific parameters from the published NOAA assessment governs transitions across classes. Recruitment is log-normal at the patch level with patch-specific marginal variances and a cross-patch correlation structure $\Sigma_\varepsilon$ recovered from biomass-survey residuals; the climate state $\theta_t$ enters through the mean, variance, and correlation of these shocks (Section 6.3). Mortality combines a natural rate $M = 0.1$ per year with fishing mortality from realized harvest. The catch production function is $\text{catch}_{k,t} = q \cdot B_{k,t}^{\gamma}$ with $\gamma = 0.40$ estimated from how harvest vary by local biomass variation. The current version uses a common elasticity across size classes. Prices are observed and are used to estimate expected revenue from each patch $k$ in week $t$, which are used in the choice model.

**The SAMS-anchored biomass panel.** The patch-level in-water biomass panel is the SAMS-anchored construction of Section 3: published PDT combined-survey totals by subarea, allocated across patches by fishing footprint and combined with dredge surveys to separate recruitment from harvest depletion, delivering biomasses consistent with the published totals at $F \approx 12\%$. Biomass shocks are the growth residuals, assembled into a cross-patch covariance matrix. Closed and zero-fishing patches need a separate allocation rule, because there is no contemporaneous fishing footprint to allocate the SAMS subarea total by, yet the closed-area conservation ratios (Table 5) are a headline result. For these patches we allocate the subarea total using the patch's *survey-based* biomass share (the dredge-survey density on the patch relative to the subarea, the same surveys used to build the shock covariance) rather than the fishing-based share. Where a patch has a recent open or access history, we use its most recent fishing-based share before closure as a cross-check, and the two agree to within the survey's sampling error on the patches where both are available. This makes the closed-patch state variable an explicitly survey-imputed quantity rather than an extrapolation from zero fishing, and it is the natural object since a closure's whole purpose is to hold biomass the fleet is not currently touching. Robustness to an equal-area (uniform) allocation within subarea is left to the next draft; it is the alternative most likely to move the most extreme closed-area ratios.

**The marginal-harvest perturbation.** The empirical counterpart of the Control FOC is computed by perturbation. In FY2014, we force every boat-trip at patch $k$ to land an additional $\delta_{kg} = 100$ kg per trip-day; the fleet then re-optimizes its spatial allocation in subsequent years under the perturbed biology. We compute $\text{MC}_k$, the marginal cost of conservation in patch $k$ or $\xi_{k,t}$, as the additional profit from this change in harvest. We compute $\text{MB}_k$ from simulating forward how the perturbation changes future stocks and

therefore future profits, inclusive of the substitution across space implied by the choice model. It is the negative of the discounted sum of future profit changes, with discount factor $\beta = 0.95$ and the horizon extending to FY2019. Monte Carlo draws over biology shocks ($n_{\text{draws}} = 100$ in the headline analysis).

**The cost parameters.** The choice model estimates area cost parameters (mean cost of traveling to any patch $k$) alongside the fixed cost of fishing in an area. We also estimate $\sigma$, the variance of the logit cost shocks, and estimate $\sigma = \$200\text{K}$ (the headline value); at this value the fleet's spatial substitution roughly matches the reduced-form displacement reach to 100–200 km documented in Section 4. The leakage term is highly sensitive to $\sigma$.

# 6 Results

We report the empirical exercise in three parts. We first document that the FY2014 regulation fails all three efficiency conditions at the margin and decompose the spatial misallocation across patches and boats. We then show how each condition responds to a different climate channel under projected mid-century biology. We close with the welfare-weighted analysis and the decoupling of static and dynamic conclusions under inequality aversion.

## 6.1 Testing the regulation in 2014

**Static intratemporal efficiency: relating MB and MC overall.** Summing across all areas in 2014, the marginal benefit of conservation exceeds the marginal cost by about 63% (Table 4): a marginal kilogram of harvest carries an expected future stock-value loss of roughly \$34 against a \$21 dock value, a \$13/kg wedge, so the 2014 harvest limits and day caps are too lax for maximizing fishery profit in present value. Leakage destroys about 17% of the marginal benefit of conservation (Table 7): restricting one area induces extra harvest elsewhere, far from one-for-one because destination grounds are more plentiful or less profitable. The same substitution cuts the marginal cost by even more (28%), so leakage on net accounts for about 13% of the static inefficiency, raising $\text{MB}/\text{MC}$ from 1.42 to 1.63.[1]

[1]Three $\text{MB}/\text{MC}$ baselines appear across the tables and refer to distinct counterfactuals: $1.42$ is the own-patch ratio that would obtain absent leakage; $1.63$ is the realized FY2014 ratio with leakage (Table 4); and $1.35$ (Table 8) is the ratio under the frozen early-period climate, before the observed changes in growth and shock covariance are applied.

**Spatial efficiency: ratio of MB to MC over space.** The aggregate masks wide heterogeneity: per-kg shadow values run from ∼\$8/kg at under-fished grounds (biomass 13M kg) to ∼\$485/kg at the most over-fished (3.2M kg), a ∼60× span within the access regime (Table 5). Some plentiful access areas and small open patches are over-restricted ($MC_k > MB_k$) while many smaller access areas could be tightened or closed; the closures sit on the highest-MB beds and are well targeted, whereas grounds just outside access areas, where substitution concentrates, are among the most over-fished, the residue of leakage from the rotational program.

**Misallocation due to spatial caps or due to boats?** The dispersion in patch-level wedges combines two misallocations: harvest in a patch is not at the stock-preserving level, or non-tradable DAS and access-area limits leave boats with different shadow prices on the same grounds. A variance decomposition of $\log \mathrm{MB}/\mathrm{MC}$ across boat-patch cells puts about three quarters of the dispersion between patches and only about 10% between boats fishing the same patch (Table 6), so the dominant source is the coarseness of the cap structure, not vessel heterogeneity. The regulation does over-restrict the most profitable boats (boat fixed effects correlate with the vessel shadow price at $+0.97$), but the decomposition implies that landing taxes or tradable permits would improve efficiency far less than re-setting harvest goals across areas.

**Dynamic intertemporal efficiency: the asset-pricing residual.** The third condition asks whether the regulation's implicit pricing of in-water stock tracks its forward asset-pricing value as the system moves through time, i.e. whether the costate equation (**??**) holds along the regulated path. In particular, we test how the marginal benefit changes as the regulation updates from year to year, given past shocks and expectations into the future. Comparing past to present marginal benefit, we can evaluate the realized residual

$$u_{k,t+1} \equiv \beta\big(-C_{k,X}(q^*_{k,t+1}, X_{k,t+1}) + \lambda_{k,t+1}\big)\big(1 + G_{k,X_k}\big) - \lambda_{k,t}$$

which has conditional expectation zero at the optimum. Computed along the simulated 2014–2019 path under the status-quo regulation and the historical biology, the average residual is about \$4.6 million (equal-weighted row of Table 10). The positive sign says the regulation implicitly under-values scallop growth as closures and access areas update year to year, though under historical growth parameters; the climate analysis below isolates how much is a failure to update.

## 6.2 Distributional incidence and the decoupling of static and dynamic

The exercise above weights vessels equally. The conservation gains do not accrue equally, however: New Bedford is 41% of fleet-wide $\mathrm{MC}$ but 52% of $\mathrm{MB}$ (an 11-pp gain in share), while the Mid-Atlantic, home to smaller, less profitable vessels and lower-income communities, is 26% of $\mathrm{MC}$ but only 14% of $\mathrm{MB}$ (a 12-pp loss). Computing equity-weighted versions of the static wedge and dynamic residual under a CRRA aggregator $U(\pi) = \pi^{1-p}/(1-p)$ (Table 10), the static wedge crosses zero at about $p = 1.5$: a planner weighting low-profit Mid-Atlantic vessels more heavily rationalizes the 2014 stringency, both because the over-fished areas are the ones those vessels target and because the restriction spares them costly travel in bad states. The dynamic residual also shrinks under inequality aversion but stays positive, so aggregate tightening, the most salient reform under equal weighting, weakens or reverses under moderate inequality aversion while the updating failure does not.

## 6.3 Changing resource growth: the climate channels

We decompose the impact of the observed changes in ecological conditions, mean growth, the variance of biomass shocks, and their spatial correlation, by simulating forward first under the early-period growth and covariance held fixed (a stationary state) and then under the observed values, so the gap measures under-reaction to a changing ocean.

**The aggregate static wedge widens sevenfold, primarily through variance and covariance.** $\mathrm{MB}/\mathrm{MC}$ moves from 1.35 in the stationary system to 1.63. We attribute this widening almost entirely to the variance and covariance channels (about equally), with falling mean growth contributing only little. The increasing uncertainty in growth and the increased spatial correlation of ecological shocks (scallops unexpectedly growing or dying together) increase the precautionary value of keeping the resource in the ocean.

**The spatial dispersion widens.** The cross-patch variance of $\log \mathrm{MB}_k/\mathrm{MC}_k$ rises by $\sim$50% under the observed changing ocean. Variance alone widens the dispersion ($+0.32$), though this is partially offset by the increased spatial correlation as more synchronized shocks make patches' precautionary responses more uniform. That increased spatial correlation is also changing the role of leakage, which is the next result.

**Leakage flips from insurance to contagion under climate.** The covariance $\mathrm{Cov}(\rho_{mk}, w_m)$ of equation (**??**), whether displaced effort reroutes toward grounds that are simultane-

ously stressed e compute it directly from the model's draw-level leakage matrix and per-patch social costs (Table 9; construction in Appendix A.8). Flow-weighted across the destination–source pairs, the aggregate covariance moves from $-\$20$K under the early-period climate to $+\$3.96$M under the observed late-period (full-climate) biology. If historical conditions prevailed, then displaced effort usually ends up in slack grounds, dampening the welfare impacts of leakage; under the warming biology it floods grounds that are stressed. This is mostly driven by the mean destination stress $\mathbb{E}[w]$, which roughly triples ($\$1.9$M $\rightarrow$ $\$5.9$M), while the draw-level correlation $\mathrm{corr}(\rho, w)$ also rises from $+0.16$ to $+0.26$, i.e. boats are becoming more sensitive to biomass shocks when substituting from closed areas. The result mostly is concentrated in the area of highest climate-induced degradation, the mid-Atlantic, where the correlation rises from $+0.08$ to $+0.32$, while the Georges Bank was already highly synchronized and barely moves ($+0.21 \rightarrow +0.23$). Leakage flows toward whichever destination is biomass-rich on a given draw, so under spatially uncorrelated shocks boats substitute to comparatively more stable areas with more plentiful (and therefore more productive) shocks. As shocks synchronize under climate change, the few productive grounds are also the high-conservation-value ones and effort concentrates there.

**The dynamic residual emerges from mean-growth degradation.** As emphasized before, the dynamic inefficiency can be driven by pre-existing static wedges or differences in expectation. Under a stationary climate, the realized residual $\mathbb{E}[u]$ is essentially zero ($-\$0.12$M, statistically indistinguishable from zero): the status-quo regulation tracks the dynamic optimum reasonably well under historical conditions. Most of that widening is from the mean main effect; variance and covariance channels contribute under \$0.3M each. The mechanism is the costate equation's persistence factor: degraded mean recruitment lowers $G_{k,X_k}$, raising the forward asset-pricing value of stock on the right-hand side of the costate equation, while the regulation's implicit shadow price (its left-hand side) holds at its historically calibrated level. This is evidence that the regulator updates, but on outdated information about ecological growth. In the language of Section **??** this is the freeze-vs-evolve test isolating the *genuine* term: the residual is zero under frozen $\theta$ and emerges only when the environment drifts, so it is a true failure to update, not static laxity propagated forward, and the reform it identifies is re-pricing the stock, not tightening caps.

# 7 Discussion and Conclusion

The empirical exercise applies three separable efficiency tests to the FY2014 spatial regulation. Statically the regulation is too lax; its spatial misallocation is between areas rather than between boats; and its implicit pricing of the stock fails the dynamic Euler condition. The existing design could be rationalized by a regulator with high preferences for redistribution to low-profit boats and by a regulator ignoring the changing ecological conditions induced by a warming ocean. In addition, the welfare consequences of leakage are changing. Over the observed warming, the substitution of activity begins to occur in more threatened areas, as opposed to more stable ones, with proximity outweighing incentives to move to more plentiful grounds and increased spatial correlation meaning all areas are likelier to degrade at once.

Three implications extend beyond the scallop fishery. First, because the conditions test different things, respond to different moments of the environment, and fail independently, distinguishing them is informative for reforming existing spatial policies in any setting where a regulator faces spatial heterogeneity under uncertainty: forest management with stochastic growth, the management of grazing areas or fire-prone areas that leak into nearby development, or water rights under hydrological variability.

Second, the variance decomposition suggests that standard tools economists suggest for efficiency improvements, i.e. those that deal with misallocation across producers like taxes or permit markets, would only go so far. The first-order problems in this fishery are with the lack of spatial coordination, though future work should confirm this by simulating what policies would look like that allow boats to equalize marginal profits to each other.

Third, the static and dynamic verdicts change dramatically under inequality aversion, emphasizing the need to consider a variety of preferences of regulators. The static wedge crosses zero at moderate aversion, because the conservation gains accrue to high-revenue vessels and a planner who weights low-revenue Mid-Atlantic vessels more heavily can read the 2014 stringency as fair. The dynamic residual falls but stays positive because the mean-growth channel that drives it runs through the biology rather than the distribution of profit across vessels. We expect this split wherever the static wedge is precautionary and the dynamic residual is mean-driven.

A design point follows for coarse instruments. The fishery's large open area, governed only by an aggregate days-at-sea budget, is less inefficient than it looks, because a single constraint lets effort flow to whichever sub-area is slack in the moment, i.e. allowing for some insurance as in equation (**??**). That turns out to be close to optimal when grounds

are weakly correlated and fails only when correlation rises and the slack disappears as the ocean warms. Whether one large open area is good design is thus regime-dependent.

Several caveats bound the results. We have yet to assess robustness of the key structural objects (the $\mathrm{MB}/\mathrm{MC}$ ratios, the leakage matrix, and the residual $\mathbb{E}[u]$) and need to increase simulations to find standard errors, especially important given sampling error in the biomass surveys. Leakage is highly sensitive to overall sensitivity of cost shocks $\sigma$, and linking reduced-form results directly rather than relying mostly on the logit assumption would be helpful. In addition, we hold regulations fixed into the future after 2014, when in reality regulators are able to respond to adjust day and harvest caps under alternative ecological shocks. Therefore future simulations should map more closely to the actual harvest rule that regulators use.

Three extensions are needed. First, incroporating the general-equilibrium ipmacts on prices could be important, and current counterfactuals hold prices as fixed. THis is a possibly important and persistent source of leakage. Reduced-form results suggest that substitution is actually less concentrated under high prices as boats spread out to scallop beds with fewer large scallops when oerall prices are high, which could mediate any sensitivty to biomass. Second, ecological spillovers could be important as the conceptual framework makes clear, and there is considerable evidence that scallop beds even some dozens of miles away can seed and amplify growth in particular regions, which could change the targeting implications. Lastly, we can elaborate on possible implicit weights of the regulation beyond just inequality in profits, such as certain smaller communities or regional preferences.

The broader contribution is methodological. Treating spatial regulation under uncertainty as a set of separable conditions, a Hotelling rule for renewable resources augmented by the cross-cell structure of allocation, turns a vague question about the value of spatial management into specific diagnostics: which condition is failing, which moment of the changing environment is driving it, and which reform would address it. Beyond that, the welfare consequences of leakage is set by the spatial correlation of the environment, and warming, by synchronizing the grounds, exacerbates the damage.

Therefore the open question is what types of regulatory deisgns are most robust to the non-stationary processes that characterize many environmental issues. : when the correlation structure that fixes the welfare sign of leakage is itself moving, the goal is not to match a spatial map to a single forecast but to build instruments that hold their value across the range of plausible climate paths, i.e. exnteding the the robust-control literature of Hansen and Sargent (2008) and Brock and Hansen (2018) to spatial policies. Our targeting results suggest that closures are already very valuable and might be extended,

though possibly with distributional consequences that a regulator would not find acceptable; future counterfactual regulations could suggest instruments that adapts to the realized state, and perhaps take account of spatial substitution directly. Designing for that non-stationary world is the central open question for spatial environmental regulation.

# References


Assunção, J., C. Gandour, and E. Souza-Rodrigues. 2019. "The Forest Awakens: Amazon Regeneration and Policy Spillover." Working Paper.

Assunção, J., R. McMillan, J. Murphy, and E. Souza-Rodrigues. 2022. "Optimal Environmental Targeting in the Amazon Rainforest." *The Review of Economic Studies*, Volume 90, Issue 4.

Bohi, D. R., and Burtraw, D. (1992). *Utility Investment Behavior and the Emission Trading Market*. Resources for the Future, Washington, DC.

Brock, W. A., and Hansen, L. P. (2018). Wrestling with uncertainty in climate economic models. *Becker Friedman Institute for Economics Working Paper No. 2019-71*, University of Chicago.

Clark, C. W. (1990). *Mathematical Bioeconomics: The Optimal Management of Renewable Resources* (2nd ed.). Wiley-Interscience, New York.

Costello, C., Gaines, S. D., and Lynham, J. (2008). Can catch shares prevent fisheries collapse? *Science*, *321*(5896), 1678–1681.

Costello, C., and Karp, L. (2004). Economic incentives to deter illegal activities in natural resource markets. *Journal of Environmental Economics and Management*, *48*(2), 1146–1157.

Earle Grupp, T., P. Mishra, M. Reynaert, and A. A. van Benthem. 2023. "An Evaluation of Protected Area Policies in the European Union." Working Paper.

Essington, T. E., Sanchirico, J. N., and Baskett, M. L. (2012). Catch shares, fisheries, and ecological performance: Evidence from the northeast United States. *Marine Policy*, *36*(3), 701–711.

Farrow, S., and Scott, M. (2012). Comparing multistage policy instruments: The case of the fishery. *Environmental and Resource Economics*, *53*(1), 41–65.

Fowlie, M., and Muller, N. Z. (2019). Market-based emissions regulation when damages

vary across sources: What are the gains from differentiation? *Journal of the Association of Environmental and Resource Economists*, *6*(3), 593–632.

Free, C. M., Thorson, J. T., Pinsky, M. L., Oken, K. L., Wiedenmann, J., and Jensen, O. P. (2019). Impacts of historical warming on marine fisheries production. *Science*, *363*(6430), 979–983.

Goulder, L. H., and Stavins, R. N. (2011). Challenges from state-federal interactions in US climate change policy. *American Economic Review*, *101*(3), 253–257.

Grafton, R. Q., Arnason, R., Bjørndal, T., Campbell, D., Campbell, H. F., Clark, C. W., Connor, R., Hannesson, R., Hilborn, R., Kirkley, J. E., Pascoe, S., Squires, D., Steinshamn, S. I., Turris, B. R., and Weninger, Q. (2006). Incentive-based approaches to sustainable fisheries. *Canadian Journal of Fisheries and Aquatic Sciences*, *63*(3), 699–710.

Greenstone, M., and Hanna, R. (2014). Environmental regulations, air and water pollution, and infant mortality in India. *American Economic Review*, *104*(10), 3038–3072.

Hansen, L. P., and Sargent, T. J. (2008). *Robustness*. Princeton University Press, Princeton.

Hansen, L. P., and Singleton, K. J. (1982). Generalized instrumental variables estimation of nonlinear rational expectations models. *Econometrica*, *50*(5), 1269–1286.

Holland, D. S. (2010). Markets, pooling and insurance for managing bycatch in fisheries. *Ecological Economics*, *70*(1), 121–133.

Lipscomb, M., and Mobarak, A. M. (2016). Decentralization and pollution spillovers: Evidence from the re-drawing of county borders in Brazil. *Review of Economic Studies*, *83*(2), 679–712.

Mallory, M. L., and Ando, A. W. (2014). Implementing efficient conservation portfolio design. *Resource and Energy Economics*, *38*, 1–18.

Markowitz, H. M. (1952). Portfolio selection. *The Journal of Finance*, *7*(1), 77–91.

Mills, K. E., Pershing, A. J., Brown, C. J., Chen, Y., Chiang, F.-S., Holland, D. S., Lehuta, S., Nye, J. A., Sun, J. C., Thomas, A. C., and Wahle, R. A. (2013). Fisheries management in a changing climate: Lessons from the 2012 ocean heat wave in the Northwest Atlantic. *Oceanography*, *26*(2), 191–195.

Newell, R. G., and Pizer, W. A. (2003). Regulating stock externalities under uncertainty. *Journal of Environmental Economics and Management*, *45*(2), 416–432.

Pindyck, R. S. (1984). Uncertainty in the theory of renewable resource markets. *Review of Economic Studies*, *51*(2), 289–303.

Pinsky, M. L., and Mantua, N. J. (2014). Emerging adaptation approaches for climate-ready fisheries management. *Oceanography*, *27*(4), 146–159.

Pizer, W. A. (2002). Combining price and quantity controls to mitigate global climate change. *Journal of Public Economics*, *85*(3), 409–434.

Reed, W. J. (1979). Optimal escapement levels in stochastic and deterministic harvesting models. *Journal of Environmental Economics and Management*, *6*(4), 350–363.

Reynaert, M., E. Souza-Rodrigues, and A. van Benthem. 2023. "The Environmental Impacts of Protected Area Policy." NBER Working Paper 31873.

Ryan, N. (2019). The competitive effects of transmission infrastructure in the Indian electricity market. *American Economic Journal: Microeconomics*, *11*(2), 33–65.

Sanchirico, J. N., Holland, D. S., Quigley, K. J., and Fina, M. (2006). Catch-quota balancing in multispecies individual fishing quotas. *Marine Policy*, *30*(6), 767–785.

Sanchirico, J. N., and Wilen, J. E. (1999). Bioeconomics of spatial exploitation in a patchy environment. *Journal of Environmental Economics and Management*, *37*(2), 129–150.

Souza-Rodrigues, E. 2019. "Deforestation in the Amazon: A Unified Framework for Estimation and Policy Analysis." *The Review of Economic Studies*, Volume 86, Issue 6.

Sudarshan, A. (2020). Droughts and the welfare of the rural poor: Evidence from In-

dia. *Journal of Development Economics*, *143*, 102419.

Weitzman, M. L. (1974). Prices vs. quantities. *Review of Economic Studies*, *41*(4), 477–491.

Weitzman, M. L. (2002). Landing fees vs harvest quotas with uncertain fish stocks. *Journal of Environmental Economics and Management*, *43*(3), 325–338.

White, C., and Costello, C. (2014). Close the high seas to fishing? *PLOS Biology*, *12*(3), e1001826.

Figure 1. Map of areas

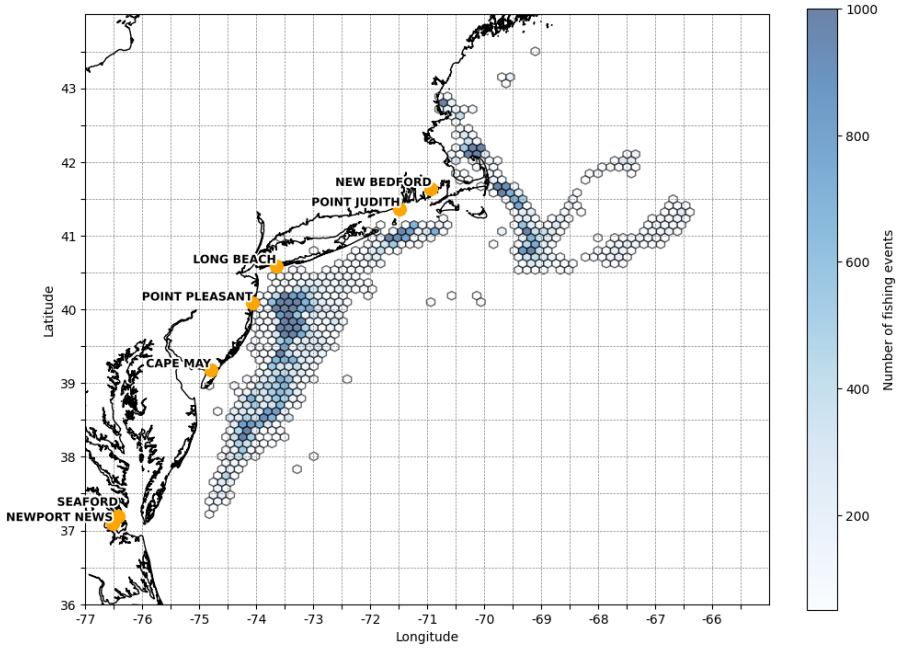


(a) Map of all harvests, 2008-2022

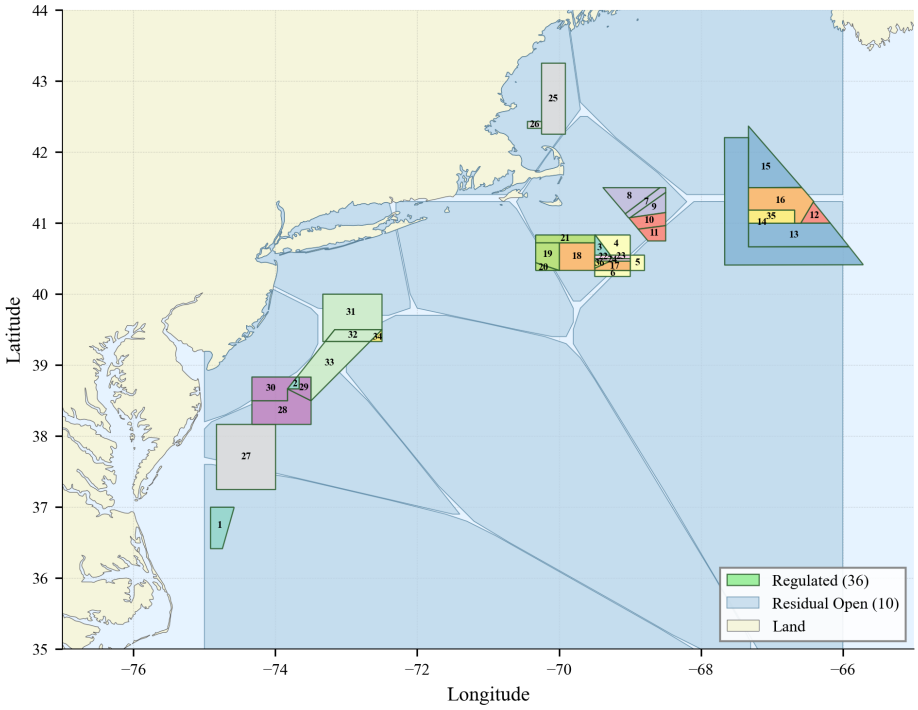


(b) Areas created for location-choice regression

*Note*: The figure shows two maps of the Northeast US scallop fishing grounds. Sub-figure (a) shows the distribution of harvests across all years, which are concentrated off of the coasts of New Jersey and Cape Cod. Sub-figure (b) summarizes our construction of areas used in the location-choice model.

Figure 2. Patch-level regression results: substitution across time

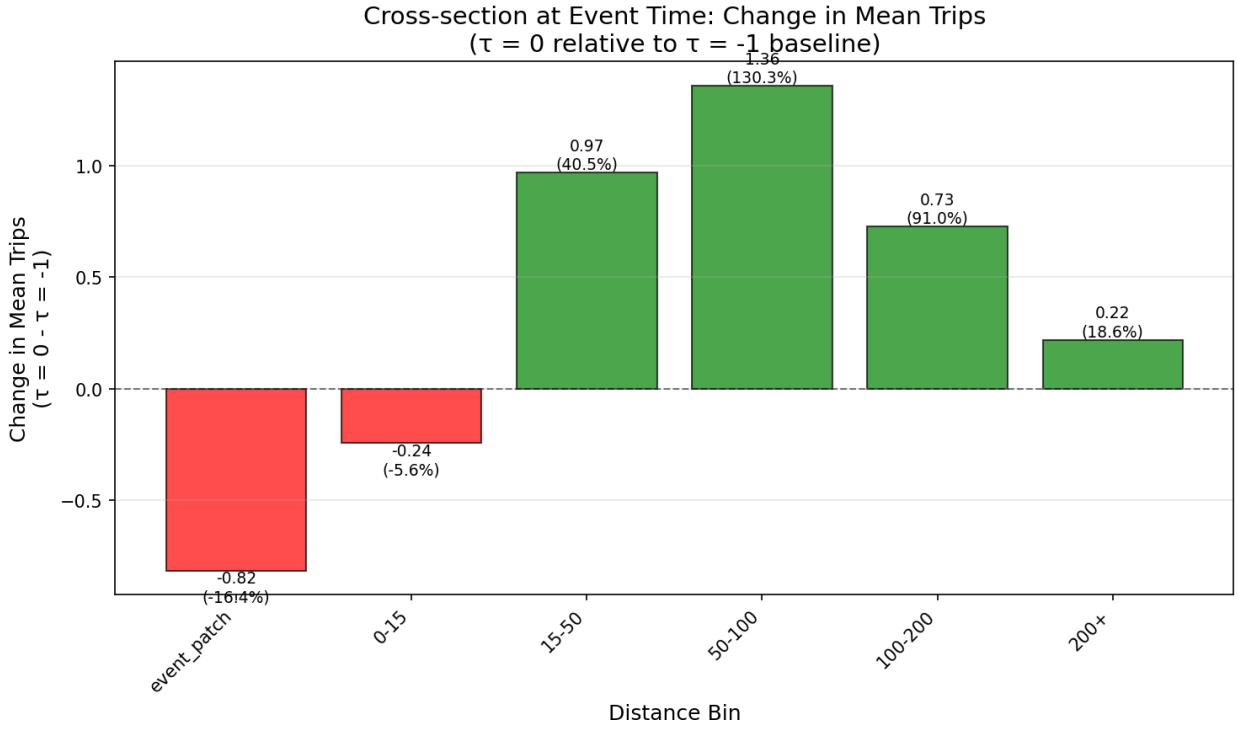


*Note*: This figure shows patch-level changes in fishing activity following a closure event, estimated using a difference-in-differences design. IT presents trip effects at the event date, normalized relative to patches more than 200 km away. The figure shows that closures lead to large declines in activity in the treated patch and substantial displacement to nearby patches, with effects decaying rapidly in distance. This pattern indicates that spatial substitution is highly local.

Figure 3. Bunching comparison

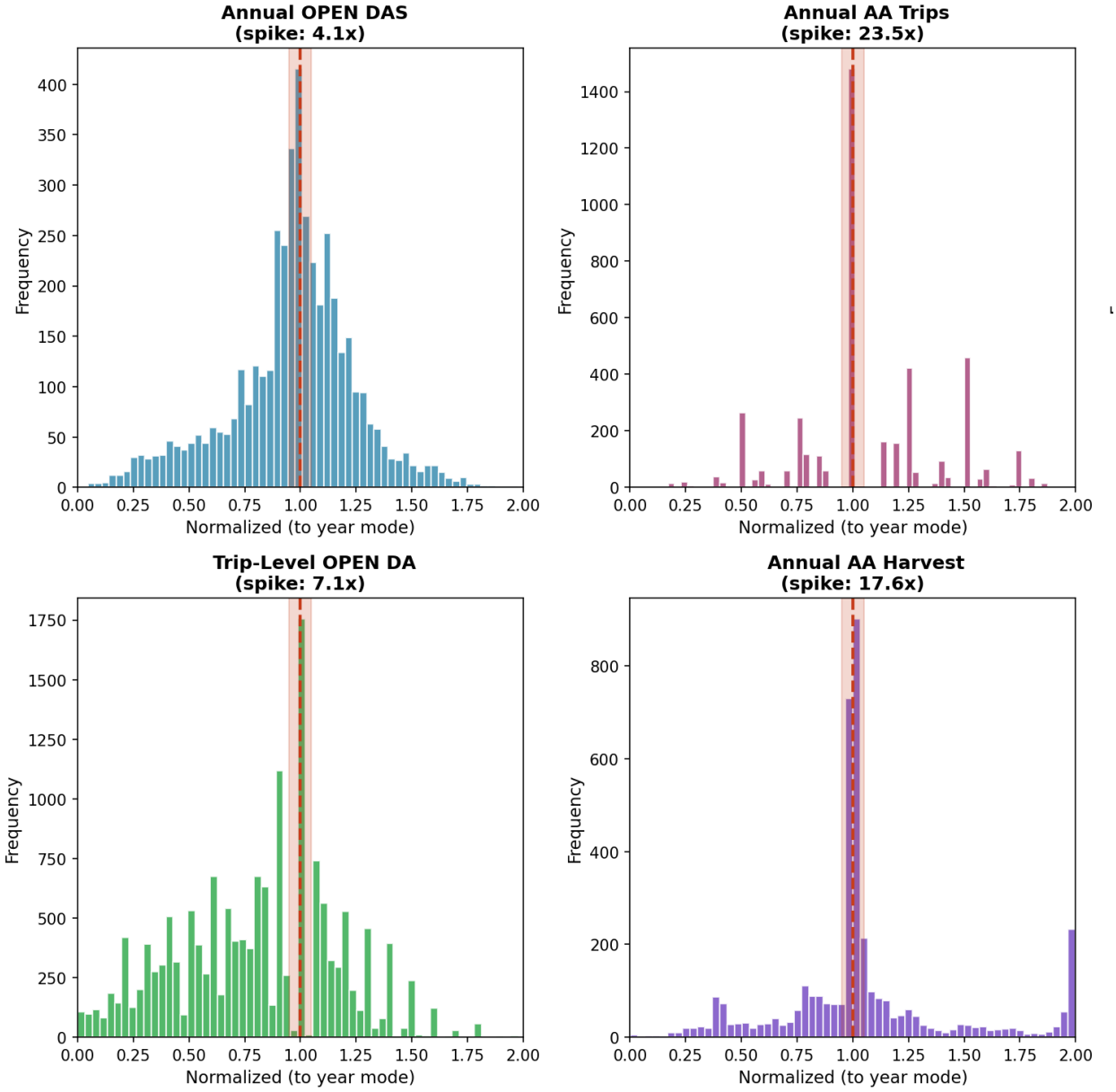


*Note*: This figure compares bunching behavior around regulatory limits under different management regimes and outcome measures. The panels plot histograms of annual or trip-level outcomes normalized by the vessel-year mode (vertical dashed line at 1), so that values near one indicate observations at the most common regulatory limit. The reported "spike" indicates the ratio of the mass at the mode to the average mass in neighboring bins, capturing the strength of bunching at the constraint. The figure shows strong bunching in access-area trips and harvest, indicating that quantity limits bind tightly in practice, while effort limits in open areas generate substantially weaker bunching. This contrast implies that the binding constraints are the harvest controls in access areas, while days at sea measures are affected by measurement error and bunching is not as clear.

Table 1. Summary Statistics

| | N | Mean | p5 | p50 | p95 |
|---|---|---|---|---|---|
| Trip duration (hrs.) | 68,001 | 73.4 | 8 | 22 | 276 |
| # fishing events/trip | 70,058 | 2.2 | 1 | 2 | 5 |
| Quantity landed/trip (lbs.) | 70,058 | 6,047 | 100 | 599 | 26,488 |
| Value landed/trip ($) | 70,058 | 57,819 | 1,066 | 6,879 | 254,638 |
| Vessel # trips/year | 4,635 | 31.2 | 2 | 16 | 128 |
| Vessel crew | 4,635 | 5.8 | 2 | 7 | 9 |
| Vessel size (GT) | 4,635 | 110 | 14 | 124 | 196 |
| # vessels/year | 9 | 515 | 490 | 500 | 597 |
| # home ports/year | 9 | 92.5 | 89 | 91 | 109 |
| Frac. revenue to New Bedford | | 0.405 | | | |
| Frac. revenue to Cape May | | 0.178 | | | |

*Note*: The table shows summary statistics from the detailed trip data available from the National Marine Fisheries Service. It aggregates across all years from 2008 to 2022. New Bedford and Cape May are the only two ports with more than 4% of the share of total revenue in the data. The first column is the sample size; the others are the mean and the 5th, 50th, and 95th percentiles respectively. Quantity landed aggregates pounds (lbs.) across all size bins in the data. Only vessels with a limited-access permit and using a scallop dredge are included. Gross tonnage (GT) is a measure of ship volume.

Table 2. Vessel-level spatial choice and margin response.

| | (1) cond. logit | (2) ext. margin | (3) int. margin |
|---|---|---|---|
| distance (100 km) | $-0.55^{***}$ | $-0.41^{***}$ | $-0.04$ |
| | (0.03) | (0.05) | (0.06) |
| closed | $-0.68^{***}$ | $-1.15^{***}$ | $-0.09$ |
| | (0.04) | (0.07) | (0.08) |
| access | $+0.71^{***}$ | $+0.60^{***}$ | $+0.02$ |
| | (0.04) | (0.06) | (0.07) |
| % effect closure vs. open | $-49\%$ | $-69\%$ | $-9\%$ |
| % effect access vs. open | $+103\%$ | $+82\%$ | $+2\%$ |
| year FE | yes | yes | yes |
| $N$ | 4,102,873 | 4,102,873 | 287,194 |

*Notes:* Column (1): trip-level conditional logit; column (2): vessel-area-year extensive-margin logit; column (3): vessel-area-year Poisson conditional on participation, so its sample is the participating vessel-area-years rather than driven by attrition. Standard errors clustered at the vessel-year level. All reported coefficients are significant at $p < 0.001$ ($^{***}$); none is significant only at the 5% or 10% level.

Table 3. Leakage sensitivity: recoup response by destination biomass and price.

| | | Trips | Harvest |
|---|---|---|---|
| *Panel A. Biomass channel:* near · post × $z$(biomass) | | | |
| patch level | closure | $+0.015$ (0.3) | $+0.194$ (1.0) |
| | opening | $+0.158$ (4.5) | $+0.826$ (5.2) |
| boat level | pooled | $+0.025$ (3.0) | $+0.153$ (5.1) |
| *Panel B. Price channel:* near · post × $z$(price) | | | |
| patch level | closure | $-0.156$ ($-4.9$) | $-0.804$ ($-5.3$) |
| | opening | $-0.062$ ($-2.8$) | $-0.505$ ($-3.3$) |
| boat level | pooled | $-0.069$ ($-7.8$) | $-0.315$ ($-11.0$) |

*Notes:* Coefficients on the triple interaction near · post × $z(\cdot)$ in the collapsed event-study of eq. (17), with $t$-statistics in parentheses; $z(\cdot)$ denotes the standardized moderator. "Recoup" is the change in activity at nearby *open* donor patches (0–50 km) relative to the treated cell's loss; donors are conditioned on being open because ∼40% of the raw ring is closed by the same event. Panel A: recoup rises with destination pre-event biomass (positive throughout; monotone increasing across destination-biomass terciles). Panel B: recoup into the local ring falls with the event-year grade-weighted price (negative throughout). Patch level is the 0.1°-cell stacked DiD (patch and year fixed effects, clustered by patch); boat level is the permit×band×event panel (boat and event fixed effects, clustered by boat). Revenue tracks harvest almost exactly and is omitted. 1,490 closure and 1,742 opening events.

Table 4. Aggregate static-efficiency wedge across the FY2014 access areas.

| | \$M | per kg |
|---|---|---|
| MC (marginal current value) | 22.0 | \$21/kg |
| MB (discounted future cost) | 35.9 | \$34/kg |
| wedge = MC − MB | $-13.9$ | $-\$13$/kg |
| MB/MC | **1.63** | |

Table 5. Cross-regulatory picture: $\mathrm{MB}/\mathrm{MC}$ by area type.

| Area type (FY2014 status) | $\mathrm{MB}/\mathrm{MC}$ | reading |
|---|---|---|
| Access, large biomass ($B > 5$M kg) | 0.4–3.7 | mixed |
| Access, small biomass ($B < 5$M kg) | 1.5–23.1 | more over-fished |
| Border areas to the rotational program | 3–206 | most over-fished |
| Open (mid-Atlantic, mixed biomass) | 0.65–62 | highly mixed |
| Closed | 1.6–106 | keep closed |

*Notes:* Ranges of $\mathrm{MB}/\mathrm{MC}$ across the patches in each category. $\mathrm{MB}/\mathrm{MC} > 1$ indicates over-fishing in 2014.

Table 6. Boat $\times$ patch variance decomposition of static-efficiency objects.

| object | between-boat | between-patch | residual | $R^2$ | corr($\alpha_{\text{boat}}$, DAS shadow) |
|---|---|---|---|---|---|
| $\log \mathrm{MC}$ | 9.3% | 75.2% | 15.6% | 84% | **+0.97** |
| $\log \mathrm{MB}$ | 19.7% | 69.2% | 11.1% | 89% | +0.84 |
| $\log(\mathrm{MB}/\mathrm{MC})$ | 10.7% | **73.3%** | 16.0% | 84% | +0.76 |

*Notes:* Two-way ANOVA on boat-patch cells with $\mathrm{MC} > 0$ and $\mathrm{MB} > 0$. Rightmost column is the Pearson correlation between the estimated boat fixed effect and each vessel's revealed shadow price.

Table 7. Decomposing effect of leakage

| component | \$M | share of total |
|---|---|---|
| *Marginal cost ($\mathrm{MC}$): year-$t$ profit response* | | |
| own-patch ($k$) | 30.6 | — |
| leakage (spatial substitution) | $-8.6$ | $-28\%$ |
| $\mathrm{MC}$ = own + leakage | 22.0 | |
| *Marginal benefit ($\mathrm{MB}$): discounted future profit response* | | |
| own-patch ($k$) | 42.0 | — |
| leakage (spatial substitution) | $-6.1$ | $-17\%$ |
| $\mathrm{MB}$ = own + leakage | 35.9 | |
| Effect of leakage on MC/MB | $1.42 \to 1.63$ | |

Table 8. Climate amplification of each efficiency condition, attributed to the mean-growth, variance, and covariance channels.

| Efficiency condition | Climate impact | Dominant climate channel | Channel attribution |
|---|---|---|---|
| Static intratemporal (MB/MC) | $1.35 \to 1.63$ | variance & covariance | variance main effect $+0.14$; covariance $+0.13$; mean $+0.01$ |
| Static spatial (var $\log \mathrm{MB}_k/\mathrm{MC}_k$) | $1.48 \to 2.28$ | mean growth & variance | 3-way interaction $+0.27$; covariance alone narrows dispersion ($-0.17$) |
| Dynamic ($\mathbb{E}[u]$) | $-\$0.12\mathrm{M} \to +\$4.55\mathrm{M}$ | mean growth | mean main effect $+\$3.95\mathrm{M}$ (87% of widening) |

*Notes:* Decomposition of how efficiency of the regulation as viewed in FY2014. The comparison estimates the marginal cost and benefit of conservation across patches when the biomass growth and shock covariance matrix from the early period (2010-2016) is fixed into the later one, versus allowing the growth parameters to change as observed. 2014 starting condition.

Table 9. Leakage flips from insurance to contagion: $\mathrm{Cov}(\rho_{mk}, w_m)$ across biology draws.

| | Early period (benign) | Late period (full climate) |
|---|---|---|
| *Panel A. Fleet aggregate (flow-weighted)* | | |
| $\mathrm{Cov}(\rho_{mk}, w_m)$ | $-\$0.02$M | $+\$3.96$M |
| character | insurance | contagion |
| robustness: $w$ from own-stock MB | $-\$0.01$M | $+\$4.00$M |
| *Panel B. Underlying moments* | | |
| $\mathbb{E}[\rho]$ (mean leakage rate) | 0.0028 | 0.0096 |
| $\mathbb{E}[w]$ (mean destination stress) | \$1.9M | \$5.9M |
| mean $\mathrm{corr}(\rho, w)$ | $+0.16$ | $+0.26$ |
| *Panel C. By destination region (mean correlation)* | | |
| Mid-Atlantic (fastest-warming) | $+0.08$ | $+0.32$ |
| Georges Bank / New England | $+0.21$ | $+0.23$ |

*Notes:* $\rho_{mk}$ is the per-draw leakage rate (share of source patch $k$'s displaced effort rerouting to destination $m$, normalized to the own-patch response); $w_m = D_m - \pi_{m,q}$ is the destination's social cost of activity, with $D_m$ the per-draw discounted future damage ($\mathrm{MB}_m$) and $\pi_{m,q}$ the deterministic marginal private profit ($\mathrm{MC}_m$). Cov taken across $n = 24$ common-random-number biology draws and flow-weighted across destination–source pairs by expected leakage flow. Negative Cov is insurance (effort flees slack grounds); positive is contagion (effort floods stressed grounds). Early period freezes growth and shock covariance at 2010–2016 values; late period uses the observed warming biology.

Table 10. Equity-weighted efficiency conditions under inequality aversion (static wedge under historical biology; dynamic residual under degraded climate).

| | Static wedge | | Dynamic residual | Leaky bucket (90/10) |
|---|---|---|---|---|
| Parameter $p$ | MB/MC | wedge \$M | $\mathbb{E}[u]$ \$M | \$ worth burning per \$1 delivered |
| 0 (equal) | 1.63 | $-13.9$ | $+4.55$ | \$0.00 |
| 0.5 | 1.38 | $-9.4$ | $+3.81$ | \$1.08 |
| 1 (log) | 1.16 | $-3.6$ | $+3.21$ | \$3.34 |
| 1.5 | 1.01 | $-0.2$ | $+2.66$ | \$8.04 |
| 2 | 0.92 | $+1.9$ | $+2.21$ | \$17.82 |
| 3 | 0.78 | $+5.4$ | $+1.62$ | \$80.64 |
| 4 | 0.66 | $+8.9$ | $+1.27$ | \$353.18 |

*Notes:* Static wedge under historical biology; dynamic residual under degraded climate. Welfare weights $w_i \propto \pi_i^{-p}$. The rightmost column reports the Okun-style leaky-bucket value implied by each $p$ to move a dollar from the top to the bottom of the income distribution ($r = \pi_{90}/\pi_{10} = 4.34$), the dollar amount the planner would destroy to transfer \$1 from the 90th-percentile vessel to the 10th-percentile vessel. Generally, a regulator with parameter $p$ should be willing to lose $1 - (\pi_L/\pi_H)^p$ to redistribute $\$1$ from percentile $H$ to percentile $L$, where $\pi_Q$ is the profit at percentile $Q$.

# A Framework derivations

This appendix collects the derivations deferred from Section 2. The first three subsections establish, on the general primitives (1)–(2), the objects the body tests: the costate as a networked asset (Section 2.3), the leakage decomposition of the wedge and the two covariances through which uncertainty enters it (Sections 2.5–2.6), and the dynamic residual (Section **??**). The remaining subsections give the *fishery specialization* — the vessel's problem, the leakage matrix and the cap and effort shadow values, the algebraic decomposition of the static shadow value, the closed-form costate, the size-structured generalization, the welfare-weighted extension, vessel heterogeneity, and the general-equilibrium price treatment — in which harvest is the activity $q$, biomass is the benefit $B$, and the marginal cost and benefit of restriction $\mathrm{MC}, \mathrm{MB}$ and the leakage share $\ell_{jk}$ of the body take the concrete forms the empirical sections estimate. Notation matches Section 2 throughout.

## A.1 The costate as a networked asset

Differentiate the value function $V_t(\mathbf{B}_t) = \max_{\mathbf{q}_t} \sum_k [\pi_k + v_k] + \beta\, \mathbb{E}_t V_{t+1}(\mathbf{B}_{t+1})$ with respect to $B_{k,t}$. By the envelope theorem the indirect effect through the optimized $\mathbf{q}_t$ vanishes, leaving the direct dividend $\pi_{k,B} + v_k'(B_{k,t}) \equiv d_{k,t}$ and the continuation effect through every law of motion $G_j$ that $B_{k,t}$ enters:

$$\lambda_{k,t} = d_{k,t} + \beta\, \mathbb{E}_t \left[ \sum_j \lambda_{j,t+1} \frac{\partial G_j}{\partial B_{k,t}} \right] = d_{k,t} + \beta\, \mathbb{E}_t \left[ \lambda_{k,t+1} G_{k,k} + \sum_{j \neq k} \lambda_{j,t+1} G_{j,k} \right],$$

which is (6). Collecting the persistence and spillover derivatives into the matrix $\widetilde{G}$ with $(\widetilde{G})_{jk} = G_{j,k}$ and stacking across $k$ gives, when $\widetilde{G}$ is locally constant, $\boldsymbol{\lambda}_t = \mathbf{d}_t + \beta\, \widetilde{G}^\top \mathbb{E}_t[\boldsymbol{\lambda}_{t+1}]$, and in a stationary state

$$\boldsymbol{\lambda} = (I - \beta\, \widetilde{G}^\top)^{-1}\, \mathbf{d}.$$

The Neumann expansion $(I - \beta \widetilde{G}^\top)^{-1} = \sum_{h \geq 0} (\beta \widetilde{G}^\top)^h$ makes the reading literal: the price of a unit of benefit at $k$ is its own dividend plus the discounted dividends of every area it feeds, at every horizon, weighted by the network paths from $k$. The fishery costate (27) below is the special case $d_k = -C_{k,X}$, $G_{k,k} = G_{k,X_k}$, with the harvest-response channel $G_{j,Q}\, \partial q_j^* / \partial X_{k,t}$ folded into the off-diagonal.

## A.2 The leakage decomposition of the wedge and the two covariances

**Leakage folds the wedge into itself.** Write the own (leakage-exclusive but network-inclusive) marginal cost and benefit of restricting activity at $k$,

$$\mathrm{MC}_k^{\mathrm{own}} = \mathbb{E}_t[\pi_{k,q}], \qquad \mathrm{MB}_k^{\mathrm{own}} = -\beta\,\mathbb{E}_t\Big[\textstyle\sum_i \lambda_{i,t+1}\,\partial G_i/\partial q_{k,t}\Big], \qquad \Delta_k^{\mathrm{own}} = \mathrm{MC}_k^{\mathrm{own}} - \mathrm{MB}_k^{\mathrm{own}}.$$

Restricting a unit at $k$ reroutes a share $\ell_{jk}$ of the displaced activity to each $j$ (the share constructed in Appendix A.5; see (8)). The rerouted activity recovers profit $\pi_{j,q}$ and re-creates damage at $j$, so the net margins are $\mathrm{MC}_k = \mathrm{MC}_k^{\mathrm{own}} - \sum_{j\neq k}\ell_{jk}\mathrm{MC}_j^{\mathrm{own}}$ and $\mathrm{MB}_k = \mathrm{MB}_k^{\mathrm{own}} - \sum_{j\neq k}\ell_{jk}\mathrm{MB}_j^{\mathrm{own}}$, and their difference returns to the same wedge,

$$\Delta_k = \Delta_k^{\mathrm{own}} - \sum_{j\neq k}\ell_{jk}\,\Delta_j^{\mathrm{own}},$$

which is (9). The MC-versus-MB asymmetry of Section 2.5 is immediate from subtracting the two cuts:

$$(\text{cut to } \mathrm{MC}_k) - (\text{cut to } \mathrm{MB}_k) = \sum_{j\neq k}\ell_{jk}\,(\mathrm{MC}_j^{\mathrm{own}} - \mathrm{MB}_j^{\mathrm{own}}) = \sum_{j\neq k}\ell_{jk}\,\Delta_j^{\mathrm{own}},$$

positive (so the ratio $\mathrm{MB}_k/\mathrm{MC}_k$ rises and restriction looks more worthwhile) exactly when the displaced activity lands at *slack* destinations, $\Delta_j^{\mathrm{own}} > 0$.

**Two covariances.** Because the policy is fixed before shocks realize, the diagnostic is run on $\mathbb{E}[\Delta_k]$, and uncertainty enters in two places. Inside the own marginal benefit, the future costate multiplies the marginal degradation, so by $\mathbb{E}[XY] = \mathbb{E}[X]\mathbb{E}[Y] + \mathrm{Cov}(X,Y)$,

$$\mathrm{MB}_k^{\mathrm{own}} = \beta\sum_i\Big(\mathbb{E}[\lambda_{i,t+1}]\,\mathbb{E}\big[-\partial G_i/\partial q_k\big] + \mathrm{Cov}\big(\lambda_{i,t+1},\,-\partial G_i/\partial q_k\big)\Big),$$

the covariance being the precautionary buffer of (10). Inside the leakage term, both $\ell_{jk}$ and the destination wedge are random, so

$$\mathbb{E}\Big[\textstyle\sum_{j\neq k}\ell_{jk}\Delta_j^{\mathrm{own}}\Big] = \sum_{j\neq k}\Big(\mathbb{E}[\ell_{jk}]\,\mathbb{E}[\Delta_j^{\mathrm{own}}] + \mathrm{Cov}\big(\ell_{jk},\,\Delta_j^{\mathrm{own}}\big)\Big),$$

which is (11). These two covariances are the entire second-moment content of the expected wedge; under deterministic biology both vanish.

**Why spatial correlation sets the sign of the leakage covariance.** The covariance $\mathrm{Cov}(\ell_{jk}, \Delta_j^{\text{own}})$ is governed by the spatial correlation of shocks. Take a symmetric $K$-area block with common shock variance $\sigma^2$ and pairwise correlation $\rho$, and split the destination wedge into a cross-area spread and an aggregate component. The spread $\Delta_j^{\text{own}} - \overline{\Delta}^{\text{own}}$, which is what lets one area be slack while another is stressed, has variance $\sigma^2(1-\rho)$; the aggregate $\overline{\Delta}^{\text{own}}$ has variance $\sigma^2[1+(K-1)\rho]/K$. Leakage that tracks slackness — sending displaced activity toward whichever area happens to have a high $\Delta_j^{\text{own}}$ — loads on the spread, producing $\mathrm{Cov} > 0$ (restriction reliably cheap) with magnitude proportional to $(1-\rho)$. Leakage forced by a system-wide threshold that binds in every area at once loads on the aggregate, producing $\mathrm{Cov} < 0$ (the displaced activity arrives where it is least wanted) with magnitude proportional to $1+(K-1)\rho$. A state-invariant reallocation has zero covariance and no uncertainty effect. This is the formal content behind Section 2.7: a rising correlation $\rho$ erodes the favorable, spread-loading hedge and feeds the adverse, aggregate-loading one, while at the same time compressing the cross-area dispersion of $\mathrm{MB}_k/\mathrm{MC}_k$ that the spatial test reads.

## A.3 The dynamic residual: inherited and genuine components

Let the regulator follow a stationary feedback policy $\mathbf{q}_t = \mathbf{h}(\mathbf{B}_t)$ that need not be optimal, and let $\lambda_{k,t}$ be the *true* marginal value of the benefit under that policy. Differentiating the value attained under $\mathbf{h}$ with respect to $B_{k,t}$, the indirect effects through $\mathbf{h}$ no longer vanish, and each carries the static wedge $\Delta_{m,t} \equiv \mathrm{MC}_m - \mathrm{MB}_m$ at the area whose activity moves:

$$\lambda_{k,t} = d_{k,t} + \beta\, \mathbb{E}_t\left[\lambda_{k,t+1} G_{k,k} + \sum_{j \neq k} \lambda_{j,t+1} G_{j,k}\right] + \sum_m \frac{\partial h_m}{\partial B_{k,t}}\, \Delta_{m,t}.$$

Moving the optimal recursion to the left defines the residual (12) and gives its inherited component, $u_{k,t} = \sum_m (\partial h_m / \partial B_{k,t})\, \Delta_{m,t}$: a weighted sum of static wedges, the weights being the policy's state-responsiveness (own laxity for $m = k$, leakage for $m \neq k$), which vanishes when $\Delta_m = 0$ everywhere. The scalar single-area version is (5).

The genuine component arises when the expectation in the recursion is formed under stale beliefs $\hat{\theta}$ rather than the true $\theta_t$. Writing $\hat{\mathbb{E}}$ for the expectation the regulator actually uses, the regulator sets its implicit shadow price to satisfy the recursion under $\hat{\mathbb{E}}$ while the true continuation value evolves under $\mathbb{E}$; subtracting the two recursions, the realized residual carries the belief gap $\beta(\hat{\mathbb{E}} - \mathbb{E})[\lambda_{k,t+1} G_{k,k} + \sum_{j \neq k} \lambda_{j,t+1} G_{j,k}]$ in addition to the inherited term. This is the boxed decomposition (13). Because $G_{k,k}$ and the conditional mean of $\lambda_{t+1}$ both move first-order with expected growth, the belief gap is dominated by

mean drift; second-moment errors enter only through the curvature of $\lambda$ and are second-order. Under a frozen environment $\hat{\mathbb{E}} = \mathbb{E}$ by construction, the genuine term is zero, and the freeze-versus-evolve comparison of Section 6.3 identifies it as the part of $\mathbb{E}[u]$ that survives stationarity.

## A.4 The vessel's problem in full

The fishery is the specialization in which the activity $q$ is harvest and the benefit $B$ is biomass $X$. The representative fleet at time $t$ takes the regulatory policy $I_t = (\{\bar{Q}_{k,t}\}_{k\in\mathcal{A}}, \bar{T}_t)$ and the state $X_t$ as given and solves

$$\max_{\{q_k\}_{k=1}^K} \sum_k \pi_{k,t}(q_k, X_{k,t}) \quad \text{s.t.} \quad q_k \le \bar{Q}_{k,t} \text{ for } k \in \mathcal{A}, \quad \sum_k T_k(q_k) \le \bar{T}_t, \quad q_k \ge 0, \tag{20}$$

with $\pi_{k,t}(q_k, X_k) = p_t q_k - C_k(q_k, X_k)$, $C_{k,q} > 0$, $C_{k,qq} > 0$, $C_{k,X} < 0$, and $T_k(q_k)$ the trip-day function mapping harvest at $k$ into days consumed. With multipliers $\xi_{k,t}, \mu_t \ge 0$ on the cap and aggregate-effort constraints, the Lagrangian is

$$\mathcal{L}_t = \sum_k \pi_{k,t}(q_k, X_{k,t}) - \sum_{k\in\mathcal{A}} \xi_{k,t}\,(q_k - \bar{Q}_{k,t}) - \mu_t \left( \sum_k T_k(q_k) - \bar{T}_t \right),$$

and the patch-level first-order condition is

$$p_t = C_{k,q}(q_k^*, X_{k,t}) + \xi_{k,t} \cdot \mathbb{1}[k \in \mathcal{A}] + \mu_t\, T_k'(q_k^*), \tag{21}$$

with complementary slackness $\xi_{k,t} \cdot (q_k^* - \bar{Q}_{k,t}) = 0$ and $\mu_t \cdot (\sum_k T_k(q_k^*) - \bar{T}_t) = 0$.

The cap rent $\xi_{k,t}$ is the marginal value to the fleet of cap relaxation: by the envelope theorem applied to optimized profit at patch $k$,

$$\frac{\partial \pi_{k,t}^*}{\partial \bar{Q}_{k,t}} = \xi_{k,t}. \tag{22}$$

The effort shadow $\mu_t$ is the analogous rent on the aggregate effort constraint, $\partial \sum_k \pi_{k,t}^* / \partial \bar{T}_t = \mu_t$. At a binding cap the rent equals the fleet's net-of-effort marginal harvest profit, $\xi_{k,t} = \pi_{k,q} - \mu_t T_k'$, which is the fishery's marginal cost of restriction $\mathrm{MC}_k$: it is what the fleet forgoes when the cap is tightened by a unit. These two shadow values are the objects the empirical exercise uses as inputs.

## A.5 The leakage matrix via the implicit function theorem

This subsection constructs the fishery leakage share $\ell_{jk}$ of (8). Treat the vessel FOC system (21) as $K$ equations in $K$ unknowns $\{q_k^*\}$, indexed by the cap configuration and the effort allowance, and ask how the harvest allocation responds to a change in the cap at one access area $k_0$, holding the rest of the policy fixed.

At the constrained patch $k = k_0 \in \mathcal{A}$ the cap binds, so $\partial q_{k_0}^*/\partial \bar{Q}_{k_0,t} = 1$. For $j \neq k_0$ the FOC at $j$ does not involve $\bar{Q}_{k_0,t}$ directly, but it involves $\mu_t$, itself a function of all caps. Differentiating (21) at $j$,

$$0 = \big(C_{j,qq}(q_j^*, X_j) + \mu_t T_j''(q_j^*)\big) \cdot \frac{\partial q_j^*}{\partial \bar{Q}_{k_0,t}} + T_j'(q_j^*) \cdot \frac{\partial \mu_t}{\partial \bar{Q}_{k_0,t}}, \tag{23}$$

and solving,

$$\boxed{\frac{\partial q_j^*}{\partial \bar{Q}_{k_0,t}} = -\frac{T_j'(q_j^*)}{C_{j,qq}(q_j^*, X_j) + \mu_t T_j''(q_j^*)} \cdot \frac{\partial \mu_t}{\partial \bar{Q}_{k_0,t}}.} \tag{24}$$

Two observations follow. First, the cross-patch derivative is proportional to $\partial \mu_t/\partial \bar{Q}_{k_0,t}$: with no binding effort constraint ($\mu_t \equiv 0$) the cross-patch derivatives are identically zero and there is no leakage — the leakage matrix exists *because of* the binding aggregate constraint. Second, relaxing the cap at $k_0$ raises harvest there, consumes days, tightens the effort budget, and raises $\mu_t$, so $\partial \mu_t/\partial \bar{Q}_{k_0,t} > 0$; with $T_j' > 0$ and the convex-cost denominator positive, the derivative is negative for $j \neq k_0$. Effort at every other patch falls when the cap at $k_0$ is relaxed; tightening the cap reverses the sign.

Aggregating, conservation of days-at-sea pins down $\partial \mu_t/\partial \bar{Q}_{k_0,t}$ implicitly through $T_{k_0}' + \sum_{j \neq k_0} T_j' \, \partial q_j^*/\partial \bar{Q}_{k_0,t} = 0$ when $\bar{T}_t$ binds. Restricting (rather than relaxing) a unit at $k_0$ reverses the sign, so the share of the restricted unit reappearing at $j$ is $\ell_{jk_0} \equiv -\partial q_j^*/\partial \bar{Q}_{k_0,t} \geq 0$ with $\sum_{j \neq k_0} \ell_{jk_0} = 1$. In the body's transparent case of a linear effort budget $T_k(q_k) = q_k$ (so $T' = 1,\ T'' = 0$), this reduces to $\ell_{jk} = (1/C_{j,qq}) / \sum_{i \neq k}(1/C_{i,qq})$, which is (8) with $\pi_{j,qq} = -C_{j,qq}$. The price-induced channel that yields an $\ell_{jk}$ of the same form is in Appendix A.13.

## A.6 The regulator's recursive problem and its first-order conditions

The regulator chooses $\{I_t\}$ to maximize expected discounted welfare. With the equal-weighted within-period flow $W(X_t, I_t) = \sum_k \pi_{k,t}^*(X_t, I_t)$ (the welfare-weighted case is in

Appendix A.11), the value function satisfies

$$V(X_t) = \max_{I_t} \left\{ W(X_t, I_t) + \beta\, \mathbb{E}_t[V(X_{t+1})] \right\}, \tag{25}$$

with $X_{k,t+1} = G_k(X_{k,t}, q^*_{k,t}, \varepsilon_{k,t+1})$ and $\varepsilon_{t+1} \sim F_\varepsilon(\cdot; \theta_t)$.

**Control FOC.** Differentiate (25) with respect to $\bar{Q}_{k_0,t}$ for $k_0 \in \mathcal{A}$. The within-period derivative is the envelope condition (22), $\partial W / \partial \bar{Q}_{k_0,t} = \xi_{k_0,t}$; the continuation derivative is $\beta\, \mathbb{E}_t[\sum_j \lambda_{j,t+1}\, G_{j,Q}\, \partial q^*_j / \partial \bar{Q}_{k_0,t}]$ with $\lambda_{j,t+1} \equiv V_{X_j}(X_{t+1})$. Setting the total derivative to zero,

$$\boxed{\xi_{k_0,t} = -\beta\, \mathbb{E}_t \left[ \sum_j \lambda_{j,t+1} \cdot G_{j,Q} \cdot \frac{\partial q^*_j}{\partial \bar{Q}_{k_0,t}} \right].} \tag{26}$$

This is the fishery form of the static condition (3): the left-hand side is the cap rent, the fishery's $\mathrm{MC}_{k_0}$; the right-hand side is the discounted future stock-value benefit summed across patches through the leakage matrix (24), the fishery's $\mathrm{MB}_{k_0}$; and the equality is the statement $\Delta_{k_0} = \mathrm{MC}_{k_0} - \mathrm{MB}_{k_0} = 0$. A lax cap leaves $\xi_{k_0,t} < \mathrm{MB}_{k_0}$, i.e. $\Delta_{k_0} < 0$.

**Costate equation.** Differentiate (25) with respect to $X_{k,t}$. The regulator has optimized $I_t$, so by envelope the indirect effect through $I_t$ vanishes, and with $\partial W / \partial X_{k,t} = -C_{k,X} > 0$,

$$\boxed{\lambda_{k,t} = -C_{k,X}(q^*_k, X_{k,t}) + \beta\, \mathbb{E}_t \left[ \sum_j \lambda_{j,t+1} \cdot \left( G_{j,X_k} + G_{j,Q} \cdot \frac{\partial q^*_j}{\partial X_{k,t}} \right) \right].} \tag{27}$$

This is the networked-asset recursion (6) in fishery form: the dividend is the cost saving $d_k = -C_{k,X}$, persistence and spillover are the biology terms $G_{j,X_k}$, and the extra harvest-response channel $G_{j,Q}\, \partial q^*_j / \partial X_{k,t}$ is the fleet's reaction to current stock. Equations (26) and (27) are structurally distinct: the first is a within-period optimality condition holding for each access area separately, the second a law of motion for the shadow value. Substituting the second into the future term of the first collapses them into a single Euler equation and hides the distinction; the empirical exercise tests the two separately, and the deviation of (27) along the actual policy is the residual of Appendix A.3.

## A.7 Algebraic decomposition of the static shadow value

The Control FOC (26) involves the expectation of a product. Applying $\mathbb{E}[XY] = \mathbb{E}[X]\mathbb{E}[Y] + \mathrm{Cov}(X, Y)$ to the bracket (treating $G_{j,Q}$ at the conditional mean and $\partial q^*_j / \partial \bar{Q}_{k_0,t}$ as deter-

ministic in $(X_t, I_t)$, so the covariance lives in $\lambda_{j,t+1}$), and using $\partial q^*_{k_0}/\partial \bar{Q}_{k_0,t} = 1$, $\partial q^*_j/\partial \bar{Q}_{k_0,t} < 0$ for $j \neq k_0$, and $G_{j,Q} < 0$,

$$\xi_{k_0,t} = \underbrace{\beta\, \mathbb{E}_t[\lambda_{k_0,t+1}] \cdot |G_{k_0,Q}|}_{\text{(a) own-patch saving}} - \underbrace{\beta \sum_{j \neq k_0} \mathbb{E}_t[\lambda_{j,t+1}] \cdot |G_{j,Q}| \cdot \left|\frac{\partial q^*_j}{\partial \bar{Q}_{k_0,t}}\right|}_{\text{(b) leakage}} + \underbrace{\beta \sum_j \mathrm{Cov}_t\Big(\lambda_{j,t+1},\, -G_{j,Q} \cdot \frac{\partial q^*_j}{\partial \bar{Q}_{k_0,t}}\Big)}_{\text{(c) precautionary covariance}}. \tag{28}$$

This is the fishery realization of the body's marginal benefit. Term (a) is the own-patch future stock-value saving. Term (b) is the leakage offset: the across-patch effort reallocation (24) preserves stock at $j \neq k_0$, so its sign convention reflects that this benefit *offsets* the conservation cost charged at $k_0$ — it is the fishery counterpart of the $-\sum_j \ell_{jk}\mathrm{MB}^{\text{own}}_j$ cut to $\mathrm{MB}_k$ in the net wedge (9). Term (c) is the own-area precautionary covariance of (10), identically zero under deterministic biology. The empirical $-17\%$ marginal-benefit leakage share is the ratio (b) / [(a) $-$ (b) $+$ (c)] in absolute value; the corresponding $-28\%$ cut to the marginal cost is the analogous reallocation in the $\mathrm{MC}_k$ margin of (9).

## A.8 Measuring the leakage covariance

The covariance $\mathrm{Cov}(\ell_{jk}, \Delta^{\text{own}}_j)$ of (11), reported in Table 9, is computed from objects the structural model already produces, with one addition to the output. In the headline decomposition the per-destination leakage response is collapsed to an aggregate scalar; we add an opt-in flag that retains, for each source patch $k$ and each Monte-Carlo biology draw, the full vector of discounted future profit changes at every destination $j$. Normalizing this vector by the own-patch response gives the per-draw leakage share $\ell_{jk}$. The destination wedge is $\Delta^{\text{own}}_j = \mathrm{MC}^{\text{own}}_j - \mathrm{MB}^{\text{own}}_j$, where $\mathrm{MB}^{\text{own}}_j$ is the per-draw marginal benefit read from the same draw and $\mathrm{MC}^{\text{own}}_j$ is the marginal private profit; because $\mathrm{MC}$ is computed from a single deterministic run, it carries no draw-level variance, so all of $\Delta^{\text{own}}_j$'s variation is the precautionary movement in $\mathrm{MB}^{\text{own}}_j$.

The draws are common-random-number aligned across the two climate corners, so $\ell_{jk}$ and $\Delta^{\text{own}}_j$ are paired draw-by-draw; we verify that the leakage matrix's own-response column reproduces the independently stored per-draw own response to within $1.2 \times 10^{-4}$. The fleet aggregate in Panel A weights each destination–source pair by its expected leakage flow, the policy-relevant object: the sign of the covariance lives in the high-flow pairs the fleet actually experiences, even where the unweighted mean covariance is mildly of the opposite sign in both corners. Two patches with $\mathrm{MB} \approx 0$ are dropped as sources and destinations, where the own-response normalization is unstable. With $n = 24$ draws the per-pair covariances carry few degrees of freedom; the regional means in Panel C pool

many pairs and are correspondingly firmer than any single pair.

## A.9 Closed-form steady-state shadow value

Under stationary policy and biology, in a steady state where $\lambda_{k,t} = \lambda_{k,t+1} \equiv \lambda_k$ and with the cross-patch terms of the costate set to zero (no biological dispersal in the persistence channel, no cross-patch dependence of harvest on stock), the Costate equation (27) collapses to $\lambda_k = -C_{k,X} + \beta\, \lambda_k\, G_{k,X_k}$, so

$$\boxed{\lambda_k \;\approx\; \frac{-C_{k,X}(q_k^*, X_k)}{1 - \beta\, G_{k,X_k}(X_k, q_k^*)}.} \tag{29}$$

This is the scalar, no-spillover special case of the networked-asset solution $\boldsymbol{\lambda} = (I - \beta\widetilde{G}^\top)^{-1}\mathbf{d}$: the numerator is the static cost saving (the dividend $d_k = -C_{k,X}$) and the denominator $(1 - \beta G_{k,X_k})$ is the inverse capitalization factor, a Faustmann-style discount weighting the infinite stream of cost savings by the persistence of stock. The approximation requires $\beta G_{k,X_k} < 1$; every object on the right is estimable from the vessel choice model and the biology model without solving a dynamic program or imposing a terminal condition.

For climate comparative statics, the closed form shows the channels through which $\theta_t$ acts on $\lambda_k$. A mean shift moves $G_{k,X_k}$ through expected biology, acting on the denominator; variance and covariance shifts do not enter the deterministic closed form and act only through the stochastic terms of the full equation (27). This is why the dynamic residual is dominated by the mean-growth channel empirically, consistent with Section 2.7.

## A.10 Size-structured generalization

The body treats $B_k$ as a scalar; for Atlantic sea scallops the stock object is a vector of size classes, and this subsection supplies the generalization the empirical model uses. Replace the scalar $X_k$ with $\mathbf{X}_k = (X_k^{\text{pre}}, X_k^{\text{small}}, X_k^{\text{med}}, X_k^{\text{u10}})^\top$ (pre-recruit, small, medium, and the highest-priced u10 class). The transition becomes $\mathbf{X}_{k,t+1} = \mathbf{G}_k(\mathbf{X}_{k,t}, q_{k,t}, \varepsilon_{k,t+1})$, and within-period profit $\pi_{k,t}(q_k, \mathbf{X}_k) = \mathbf{p}_t^\top \mathbf{q}_k - C_k(q_k, \mathbf{X}_k)$ with a size-specific price vector.

The costate becomes a matrix recursion. With $\boldsymbol{\lambda}_{k,t} = \nabla_{\mathbf{X}_k} V$ and $(\mathbf{G}_{k,X}^{\text{class}})_{m,m'} = \partial X_{k,t+1}^{(m)} / \partial X_{k,t}^{(m')}$ (positive off-diagonals capturing maturation),

$$\boldsymbol{\lambda}_{k,t} = -\mathbf{C}_{k,X} + \beta\, \mathbb{E}_t\big[(\mathbf{G}_{k,X}^{\text{class}})^\top\, \boldsymbol{\lambda}_{k,t+1}\big], \qquad \boldsymbol{\lambda}_k \approx (\mathbf{I} - \beta\, \mathbf{G}_{k,X}^{\text{class}})^{-1}\,(-\mathbf{C}_{k,X}),$$

the matrix analogue of (29) (and the within-patch, multi-class analogue of the networked-

asset inverse). Two facts follow. The shadow value of a marginal small scallop inherits a *maturation premium*: it is augmented by the discounted probability that the scallop matures into the higher-priced classes, summed over horizons along the maturation path. And the own-patch term (a) of (28) carries this premium, while the leakage term (b) is unchanged in structure because maturation operates within a patch. The empirical signature is a hump-shaped impulse response of profit to a marginal harvest, peaking one to two years after the perturbation rather than on impact — a pattern impossible in a scalar-stock model and direct evidence for the size-structured costate.

## A.11 Welfare-weighted extension

Replace the equal-weighted aggregator $W = \sum_k \pi_k^*$ with a weighted CRRA aggregator

$$W = \sum_i w_i \, U(\pi_i^*), \qquad U(\pi) = \pi^{1-p}/(1-p), \qquad U'(\pi) = \pi^{-p}, \tag{30}$$

where $i$ indexes vessels (extending Appendix A.12) and the inequality-aversion parameter is $p \geq 0$ (the correlation $\rho$ of the preceding subsections is unrelated). Natural weights are $w_i \propto \text{revenue}_i^{-p}$, placing larger weight on lower-revenue vessels.

The Control FOC (26) becomes $\xi_{k_0,t} \cdot \overline{U'}_{k_0} = -\beta \, \mathbb{E}_t[\sum_j \lambda_{j,t+1} \, G_{j,Q} \, \partial q_j^* / \partial \bar{Q}_{k_0,t}]$, where $\overline{U'}_{k_0} = \sum_i w_i U'(\pi_i^*) \cdot (\text{share of vessel } i\text{'s revenue at } k_0)$ is the welfare-weighted marginal utility at the perturbed patch. The structural form of (28) is preserved; what changes is the dispersion of vessel weights across patches.

Two implications follow, and together they are the static/dynamic decoupling of Section 2.8. First, the static wedge is planner-specific. A redistributive planner (higher $p$) weights the effort-constrained high-revenue vessels less; if the conservation gains from cap tightening accrue disproportionately to those vessels, as Section 6 documents, $\overline{U'}_{k_0}$ shrinks more than the right-hand side and the welfare-weighted wedge crosses zero at some $p > 0$ (near $p \approx 1.5$ empirically). Second, the Costate equation (27) reweights through $-C_{k,X}$ and the forward $\lambda_{j,t+1}$, both of which propagate through the biology rather than the cross-vessel distribution of profit; the dynamic residual is reweighted in magnitude but does not pick up the asymmetry the Control FOC does, and it remains positive at every plausible $p$. The static case is planner-specific while the dynamic case is planner-invariant in sign.

## A.12 Vessel heterogeneity

The representative-fleet treatment extends to a heterogeneous fleet $i = 1, \ldots, N$ without changing the structural form. Vessel-specific cost functions $C_{i,k}$, trip-day functions $T_{i,k}$, and effort shadows $\mu_{i,t}$ replace the representative versions, and the patch cap is split across vessels by the institutional allocation rule, $\bar{Q}_{i,k,t}$. The vessel-level FOC is

$$p_t = C_{i,k,q}(q^*_{i,k}, X_k) + \xi_{i,k,t} \cdot \mathbb{1}[k \in \mathcal{A}] + \mu_{i,t}\, T'_{i,k}(q^*_{i,k}), \tag{31}$$

and the vessel-level leakage matrix is identical in structure to (24), $\partial q^*_{i,j}/\partial \bar{Q}_{i,k_0,t} = -T'_{i,j}/(C_{i,j,qq} + \mu_{i,t} T''_{i,j}) \cdot \partial \mu_{i,t}/\partial \bar{Q}_{i,k_0,t}$. Aggregate $\xi_{k,t}$ and $\mu_t$ are harvest- or effort-share-weighted aggregates of the vessel-level shadows. The empirical implementation in Section 6.1 identifies this structure through a two-way fixed-effect decomposition: the boat effect on the log per-cell shadow value isolates the vessel-specific effort shadow (correlated $+0.97$ with the directly observed effort shadow), and the patch effect isolates the coarseness of the cap structure.

## A.13 General-equilibrium prices

The development above treats the ex-vessel price $p_t$ as exogenous; making it endogenous through inverse demand $p_t = P(\sum_k Q_{k,t})$ is the price-induced leakage channel named in Section 2.3 and yields an $\ell_{jk}$ of the same form as the effort-budget channel. The vessel FOC becomes $P(\cdot) + Q_{k,t} P'(\cdot) = C_{k,q} + \xi_{k,t} + \mu_t T'_k$, and the implicit-function analysis of Appendix A.5 acquires a price term,

$$\left.\frac{\partial q^*_j}{\partial \bar{Q}_{k_0,t}}\right|_{GE} = \left.\frac{\partial q^*_j}{\partial \bar{Q}_{k_0,t}}\right|_{\text{effort}} + \frac{P'(\cdot)}{C_{j,qq} + \mu_t T''_j} \cdot \frac{\partial \sum_k Q_{k,t}}{\partial \bar{Q}_{k_0,t}}.$$

The price channel reinforces the effort channel: tightening the cap at $k_0$ lowers aggregate harvest, raises $p_t$, and raises harvest at every other patch, so the two push the displaced activity in the same direction. They separate empirically only with demand variation independent of supply regulation; the analysis in the paper holds $p_t$ fixed and so subsumes the price-channel leakage into the estimated $\ell_{jk}$, understating total leakage relative to a full general-equilibrium treatment.